Chinese Chemical Letters 37 (2026) 111489

Contents lists available at ScienceDirect

Chinese Chemical Letters

journal homepage: www.elsevier.com/locate/cclet

Design, synthesis, and optimization of MXene- and MOF-based materials for 3D printed energy storage devices and beyond

Huijie Zhou[a,b], Mutawara Mahmood Baig[b,c], Shunyu Gu[b], Wenjiang Zou[a], Jing Zhang[a], Fei Dou[b], Jiang Xu[a], Lvzhou Li[a], Yizhou Zhang[c,*], Huan Pang[a,b,*], Jianning Ding[a,*]

[a] Institute of Technology for Carbon Neutralization, Yangzhou University, Yangzhou 225127, China
[b] School of Chemistry and Chemical Engineering, Yangzhou University, Yangzhou 225009, China
[c] Institute of Advanced Materials and Flexible Electronics (IAMFE), School of Chemistry and Materials Science, Nanjing University of Information Science and Technology, Nanjing 210044, China

ARTICLE INFO

Article history:
Received 23 January 2025
Revised 17 June 2025
Accepted 18 June 2025
Available online 24 June 2025

Keywords:
MXene
MOF
Mixed inks
3D printing
Energy storage devices

ABSTRACT

MXene and metal-organic frame (MOFs) are emerging as transformative materials in the field of energy storage and conversion. While MXene excel in conductivity, tunable surface chemistry, and flexibility, MOFs bring complementary benefits with their tunable porosity and structural versatility, enabling the design of hybrid systems with enhanced functionalities. However, challenges such as material stability, structural integrity, and ink formulation must be addressed to fully integrate these materials into 3D printing technologies. This review elucidates cutting-edge material design frameworks for MXene- and MOF-integrated 3D-printed architectures, emphasizing their transformative roles in advancing energy storage/conversion systems. We provide a systematic evaluation of additive manufacturing compatibility and multidisciplinary optimization strategies spanning ink rheology, hierarchical structure engineering, and interfacial electrochemistry to enhance device performance metrics. Additionally, by analyzing the key advantages and limitations of MXene- and MOF-based materials, we examine their role in overcoming current challenges in electrochemical energy storage devices. Finally, we provide insights into future prospects, presenting a roadmap for integrating MXene and MOFs into scalable 3D printing technologies, which will enable breakthroughs in sustainable and high-performance energy devices.

© 2026 Published by Elsevier B.V. on behalf of Chinese Chemical Society and Institute of Materia Medica, Chinese Academy of Medical Sciences.

1. Introduction

With rapid technological advancements and the increasing demand for sustainable solutions, the development of advanced materials for energy storage and conversion has become a prominent area of research [1–7]. Among various innovative approaches, three-dimensional (3D) printing stands out for its ability to design complex, high-performance structures with remarkable flexibility, adaptability to different materials, and rapid prototyping capabilities [8–10]. As a frontier in materials science, 3D printing technology not only enables the construction of complex and intricate microstructures but also plays an important role in the design of customized and high-performance energy storage devices.

MXene and metal organic frameworks (MOFs) are two emerging materials with unique physical and chemical properties, that make them well-suited for 3D printing applications in energy storage [11–14]. MXene, a family of two-dimensional transition metal carbides, nitrides, or carbonitrides, are distinguished by their high electrical conductivity, versatile surface chemistry, and mechanical robustness [15–17]. These attributes position MXene as ideal candidates for high-energy-density devices, where they deliver outstanding performance and stability [18,19]. In contrast, MOFs are known for their highly tunable porous structures and excellent chemical stability, which have made them valuable in gas storage [20–22], separation [23,24], and catalysis applications [25,26]. Although MXene and MOF-based materials have distinct chemical properties, a comprehensive understanding of their respective roles in 3D printing mechanisms, coupled with strategic integration through comparison, combination, and future outlooks, can address common challenges in energy device engineering, such as charge transport and compatibility conflicts. The integration of MXene and MOF materials with 3D printing technology opens up new possibilities for the creation of complex multifunctional structures, thereby advancing the development of next-generation energy storage devices. Integrating MXene and MOFs with 3D

* Corresponding authors.
E-mail addresses: yizhou.zhang@nuist.edu.cn (Y. Zhang), panghuan@yzu.edu.cn (H. Pang), dingjn@yzu.edu.cn (J. Ding).

https://doi.org/10.1016/j.cclet.2025.111489
1001-8417/© 2026 Published by Elsevier B.V. on behalf of Chinese Chemical Society and Institute of Materia Medica, Chinese Academy of Medical Sciences.

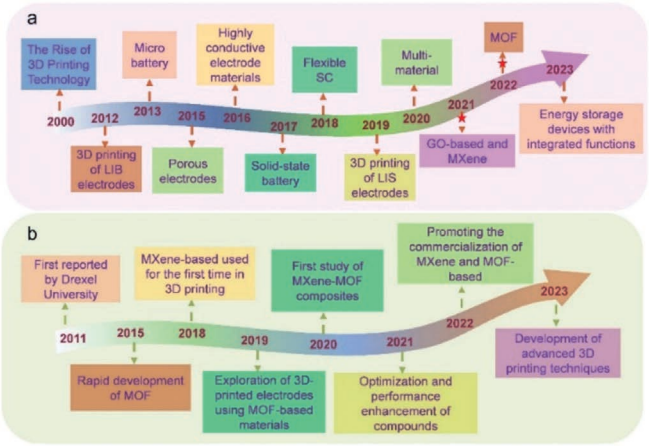


Fig. 1. (a) Development timeline of 3D printing materials employed in electrochemical energy storage devices (EESDs). (b) Timeline showcasing the evolution of MXene- and MOF-based materials in 3D-printed energy storage applications.

printing technology has opened avenues for creating complex and multifunctional structures that advance next-generation energy storage devices [27–30].

However, the successful 3D printing of MXene- and MOF-based materials depends largely on ink formulation. The rheological properties, stability, and printability of the ink directly influence the precision, structural integrity, and overall performance of the final printed devices [31–33]. Therefore, developing inks with optimal flow characteristics and uniform dispersion is essential for compatibility with various 3D printing techniques, such as stereolithography (SLA) and fused deposition modeling (FDM) [34–36]. This remains a significant research challenge, as current efforts strive to overcome these technical barriers to unlock the full potential of these materials.

Recent studies have demonstrated the effectiveness of 3D printed MXene- and MOF-based structures in energy storage and conversion devices, including supercapacitors [37,38], batteries [39], and catalysis [40], showcasing their enormous potential for significantly enhancing device performance and efficiency [41]. Fig. 1 illustrates the advances and diverse applications of MXene- and MOF-based materials in 3D printing, showcasing how these materials have been developed and optimized for various applications. It highlights their potential in creating complex, high-performance structures, particularly in energy storage, catalysis, and functional devices. This combination of MXene and MOFs with 3D printing technologies underscores their versatility and transformative impact, paving the way for innovative designs that address critical needs in energy and environmental applications.

However, despite the progress, there remains a gap in the literature on a comprehensive review that specifically addresses the critical aspects of ink formulation and the material properties essential for the effective use of MXene and MOFs in 3D printing. This article aims to bridge that gap by providing an in-depth analysis of recent advancements in 3D printing with MXene and MOF-based materials, with a particular focus on ink formulation strategies and their practical applications in energy storage and conversion. Specifically, this review provides a comprehensive analysis of the design, synthesis, and optimization of MXene- and MOF-based materials for 3D printed energy storage devices for the first time. We propose strategies to enhance the performance of MXene-MOF-based materials by optimizing ink formulation and device architecture. Additionally, we optimize the parameters for 3D printing of MXene- and MOF-based materials to improve the electrochemical performance of energy storage devices. Through a thorough assessment of the current research landscape and its challenges, we aim to provide valuable insights and guidance for future research, encouraging the widespread application of these materials in sustainable energy technologies and real-world solutions.

2. Applications of MXene-based functional materials in 3D printing

The integration of MXene-based materials into 3D printing has unlocked a range of new possibilities in advanced manufacturing and functionalization, owing to their exceptional physical and chemical properties. These features enable innovative breakthroughs in printing accuracy, material stability, and structural functionality. In this section we provide a detailed overview of the key advancements in designing and optimizing MXene inks, focusing on regulating ink rheology, enhancing dispersion stability, and improving material performance for complex 3D structures. Various 3D printing techniques, including SLA and FDM, are explored, alongside strategies for tailoring MXene inks to suit specific applications. Additionally, we address the successes and challenges faced in incorporating MXene-based materials into electrochemical devices, sensors, and other functional systems. By highlighting both innovations and potential limitations, we offer valuable insights for the future integration of MXene in cutting-edge 3D printing technologies, guiding their effective use in next-generation applications.

2.1. Pure MXene: Additive-free approaches for high-precision printing

A significant breakthrough in MXene based 3D printing is the development of additive-free inks, which eliminate the need for binders and other additives that could compromise the inherent properties of MXene. This approach has been particularly successful in direct printing techniques [39], allowing for the creation of flexible, high-precision microstructures without the need for additional processing (Fig. 2a) [42]. These advancements highlight the critical role of ink formulation in achieving both precision and functionality in printed devices. For example, the use of 2D $Ti_3C_2T_x$ (MXene) inks has opened new possibilities for the fabrication of intricate microscale devices [43], enabling the direct printing of MXene structures with enhanced mechanical integrity and accuracy (Fig. 2b). Such developments open the door to more efficient and accurate production of functional devices.

Combining cold-trap environments with freeze-drying techniques has proven to be an effective strategy for advancing MXene electrode design. This method enables the fabrication of porous, high-surface-area MXene structures that optimize ion transport pathways, particularly benefiting applications like aqueous zinc-ion batteries (ZIBs) [44]. By preventing the common issue of self-stacking among MXene layers, this approach preserves both conductivity and electrochemical performance while enhancing overall structural stability. Additionally, the integration of freeze-drying with 3D printing has led to the creation of MXene aerogels that exhibit remarkable porosity and mechanical integrity. These aerogels maintain their structural coherence and functional properties even under operational stress, addressing one of the most critical challenges in developing stable, high-performance MXene-based devices for advanced energy storage. This strategy has significant potential for the design of energy storage devices requiring both high conductivity and structural robustness [45,46].

Template-assisted 3D printing methods have enabled the fabrication of $Ti_3C_2T_x$ MXene microlattices with customized structures [47], enabling precise control over the architecture of printed materials and expanding their use across various fields (Fig. 3a). Such precise architectural control allows for the optimization of material properties to meet specific application requirements. Recent

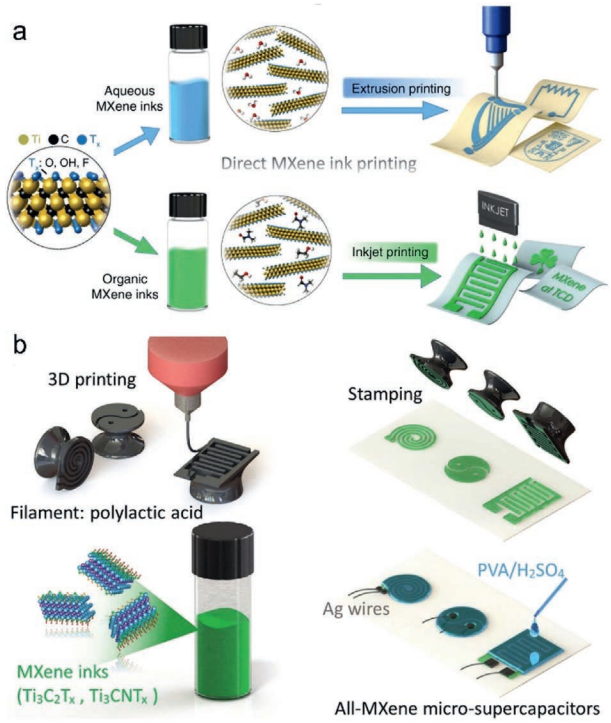


Fig. 2. Innovations in additive-free MXene inks for high-precision 3D printing. (a) Schematic illustration of direct MXene ink printing, enabling the creation of flexible microstructures while preserving MXene inherent properties for improved precision and functionality. Reprinted with permission [42]. Copyright 2019, Nature Publishing Group. (b) Fabrication of all-MXene-based MSCs using the stamping strategy, demonstrating the capability of 2D $Ti_3C_2T_x$ inks to produce intricate, mechanically robust structures with high accuracy. Reprinted with permission [43]. Copyright 2018, Wiley-VCH.

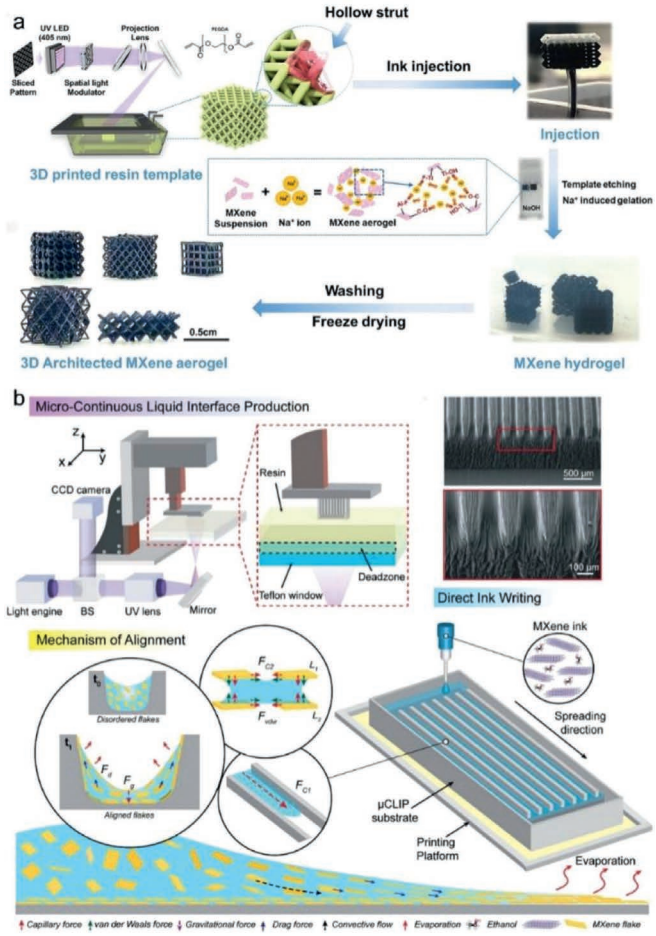


Fig. 3. Template-assisted and customized 3D printing of $Ti_3C_2T_x$ MXene microlattices. (a) Schematic illustration of 3D printing of MXene microlattices with customized structures, demonstrating precise control over material architecture and its expanded applications. Reprinted with permission [47]. Copyright 2022, American Chemical Society. (b) Schematic of hybrid 3D printing combining MXene nanosheet alignment for 3D micropatterning, enhancing structural integrity and mechanical strength. Reprinted with permission [48]. Copyright 2021, American Chemical Society.

advancements, such as aligning $Ti_3C_2T_x$ MXene nanosheets during 3D micropatterning with 3D printing, have further enhanced the structural integrity and mechanical strength of these materials (Fig. 3b) [48]. These techniques demonstrate the potential of 3D printing to engineer materials with complex geometries and customized functionalities, emphasizing the strategic value of this technology in advancing MXene-based applications.

A deep understanding of the rheological characteristics of MXene dispersions is essential for optimizing the 3D printing process. A comprehensive analysis of the flow behavior of 2D MXene dispersions has provided valuable insights into processing these materials effectively. By tailoring the rheology of MXene inks, researchers can enhance printability and achieve the desired structural properties in final printed products (Fig. 4a) [49]. Additionally, the microscale curling and alignment of $Ti_3C_2T_x$ MXene through the confinement of aerosol droplets further highlights the importance of rheology in shaping material behavior during printing (Fig. 4b) [50]. These findings highlight the critical importance of controlling the flow characteristics of MXene inks to achieve precision in printed structures.

The progress in 3D printing technologies for MXene-based materials has unlocked exciting opportunities for their integration across a range of fields. For example, Fu *et al.* [51] engineered 3D-architected gyroid MXene scaffolds for micromechanical sensing, illustrating the potential of MXene in sensing applications. The ability to fabricate complex 3D architectures significantly enhances the functional versatility of MXene, enabling their integration into multifunctional devices. Future research should continue to explore the synergies between MXene materials and 3D printing technologies. Key opportunities include developing novel MXene composites, optimizing printing processes for large-scale production, and expanding the range of applications for MXene-based printed materials.

In conclusion, the integration of MXene materials into 3D printing technologies represents a significant advancement in material science and advanced manufacturing. Innovations in ink formulation, printing techniques, and material design will drive further progress in this exciting field, leading to the development of next-generation devices with enhanced capabilities. As research continues to address current challenges and explore new opportunities, MXene are set to play a pivotal role in shaping the future of 3D printing applications across a range of industries.

2.2. Surface modification strategies for enhanced MXene properties

Recent advancements in 3D printing with MXene-based materials have focused on enhancing their performance by addressing key challenges, including self-stacking and flexibility limitations. Below, we highlight innovative modifications to MXene that significantly enhance their functional capabilities and structural resilience, paving the way for more robust and versatile applications.

One of the primary challenges in MXene-based 3D printing is the natural tendency of MXene nanosheets to self-stack, which can reduce active sites, impede ion transport, and lower electrochem-

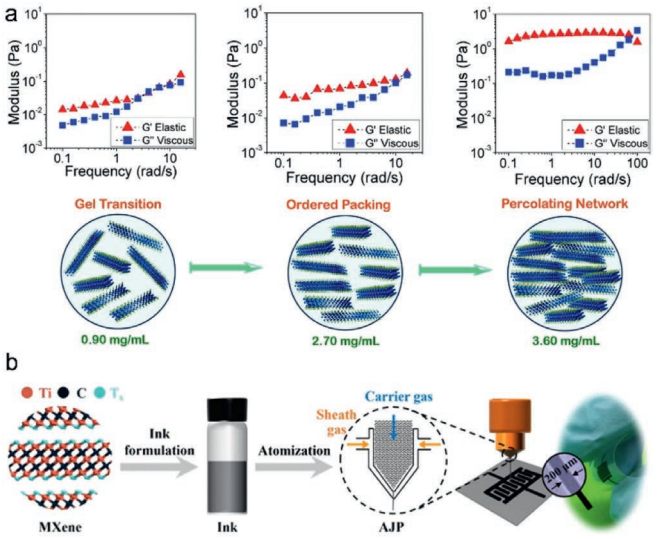


Fig. 4. Rheological characterization and printing process of MXene inks. (a) Plots showing viscoelastic measurements conducted on MXene flake suspensions at various concentrations, highlighting the rheological behavior and its impact on processing. Reprinted with permission [49]. Copyright 2018, American Chemical Society. (b) Schematic illustration of the Aerosol Jet Printing (AJP) process used for creating MXene patterns, demonstrating the role of rheology in precise patterning. Reprinted with permission [50]. Copyright 2021, American Chemical Society.

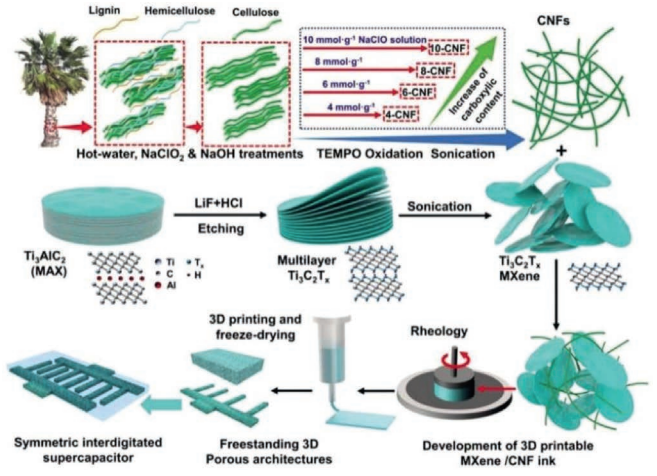


Fig. 5. Schematic illustration of the manufacturing strategies for 3D printing freestanding, hierarchically porous MXene/CNF 3D architectures. The design incorporates physical spacers, and optimized ink rheology to fabricate symmetric interdigitated supercapacitors with enhanced porosity, mechanical stability, and structural integrity. Reprinted with permission [52]. Copyright 2021, Wiley-VCH.

ical performance. Recent studies have addressed this issue by incorporating cellulose nanofibers with $Ti_3C_2T_x$ MXene which act as physical spacers between MXene layers [52]. These nanofibers effectively prevent self-stacking, preserve porosity, enhance mechanical properties, and stabilize the structure, enabling more efficient ion transport and higher electrochemical performance. This approach has been further extended to hydrogel electrolytes, where cellulose nanofibers form a flexible, supportive matrix that maintains layer separation, increases flexibility, and improves durability (Fig. 5). Additionally, optimizing the rheological properties of MXene/cellulose nanofiber inks has been essential to ensure smooth extrusion and precise layer deposition [53], which prevents self-stacking while maintaining the structural integrity of printed objects. These strategies, including the addition of physical spacers, creation of supportive matrices, and optimization of ink

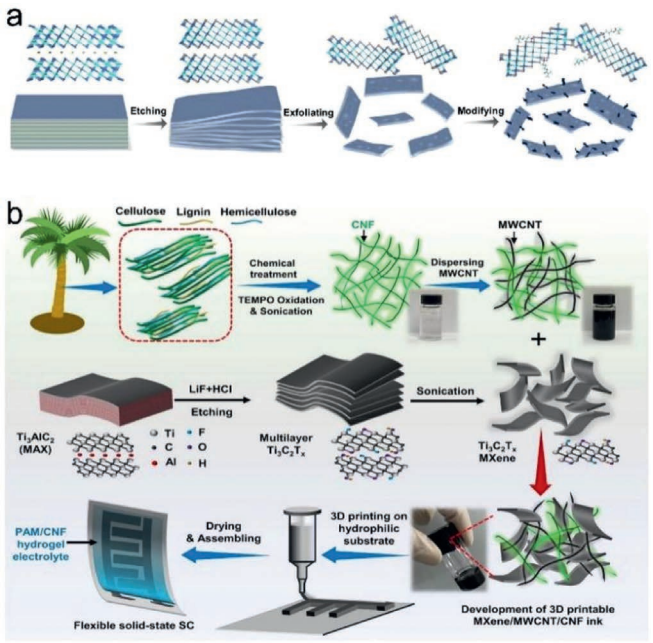


Fig. 6. Fabrication and modification of MXene-based flexible structures. (a) Schematic illustrating the sequential processing steps involved in fabricating MXene-coated polyurethane elastomer nanosheets, designed to enhance the mechanical strength and flexibility of the resulting structure for flexible electronics. Reprinted with permission [55]. Copyright 2022, Elsevier. (b) Schematic illustration of 3D printing of a FSC device, using MXene composites, demonstrating the role of MXene-based ink in achieving high structural integrity and optimized flow properties during printing. Reprinted with permission [53]. Copyright 2024, The Royal Society of Chemistry.

properties, represent significant advancements in overcoming self-stacking challenges. Gurbuz *et al.* [54] aims to address the low oxidation resistance and re stacking issues of MXene based materials by combining nitrogen and sulfur co doped V_2C MXene nanoflowers with porous multi walled carbon nanotubes. They enhance the performance of MXene-based 3D printing, opening up new possibilities for robust and efficient applications, such as energy storage devices.

Enhancing flexibility and mechanical stability of MXene: In the realm of 3D printing and flexible electronics, MXene have gained significant attention for improving the mechanical strength and flexibility of printed structures. A notable development uses MXene-coated polyurethane elastomers [55], to enhance the mechanical integrity and structural stability in flexible materials (Fig. 6a). This modification highlights the potential of MXene to significantly improve the performance of flexible materials, particularly in improving durability and functionality. Additionally, recent investigations into $Ti_3C_2T_x$ MXene and its composites have explored their effectiveness in solid-state supercapacitors [53]. These studies explore how MXene-based composites influence ink rheology and material stability during 3D printing, further advancing the potential of MXene in energy storage applications (Fig. 6b). These findings underline the critical role of MXene in enhancing the flexibility and performance of printed materials. The strategies used to optimize MXene modifications for 3D printing not only address inherent material limitations but also pave the way for the development of durable, flexible, and high-performance materials suitable for advanced energy storage and wearable electronics.

2.3. MXene composite functional materials: Performance for diverse applications

This section highlights the key progress in MXene-based composites, particularly their incorporation into hydrogel, biomate-

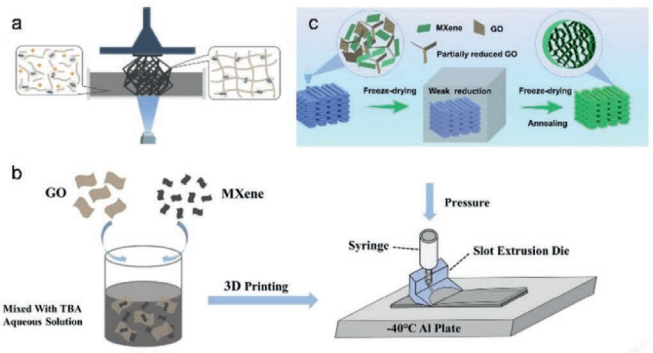


Fig. 7. (a) Illustration of 3D printing of the MXene nanocomposites using an LCD pinter. Reprinted with permission [56]. Copyright 2022, American Chemical Society. (b) Schematics of the 3D printing MXene/graphene hybrid aerogels processes. Reprinted with permission [58]. Copyright 2022, the Royal Society of Chemistry. (c) Schematic illustration of the fabrication process of hierarchical MXene/RGO scaffolds. Reprinted with permission [59]. Copyright 2022, The Royal Society of Chemistry.

rial, other functional materials, emphasizing their enhanced performance and diverse applications.

MXene-based nanocomposites have demonstrated outstanding toughness and thermal stability, particularly when prepared using 3D printing technology. These properties make MXene ideal candidates for applications requiring heat resistance and durability (Fig. 7a) [56]. Furthermore, the introduction of 4D printing technology has further expanded the potential of MXene composites, enabling the development of smart materials capable of dynamically altering their shape in response to external stimuli. This innovation opens new avenues for creating responsive systems and adaptive materials for use in diverse fields, such as robotics and smart textiles [57].

MXene exhibit tremendous potential when combined with other materials, such as graphene, to enhance electromagnetic interference (EMI) shielding capabilities. For example, the development of MXene/graphene hybrid aerogels and reduced graphene oxide (rGO) structures has demonstrated the effectiveness of these composites in achieving broadband EMI shielding (Figs. 7b and c) [58,59]. By incorporating MXene to enhance electrical conductivity, GO to improve dispersibility and rheological properties, and lignosulfonate to strengthen adhesion and self-assembly capability, the ink formulation is optimized for improved stability and ion transport efficiency. Furthermore, rheological testing reveals that the ink exhibits shear-thinning behavior, where its high viscosity effectively preserves the integrity of the 3D-printed structure. Consequently, this formulation enables the stable fabrication of thick electrodes with vertically aligned porous architectures, ensuring enhanced electrochemical performance [60]. The integration of MXene with graphene enhances both conductivity and structural integrity, making these materials highly suitable for electronic devices and protective coatings. In addition, 3D printing technology has been used to construct MXene decorated carbon black based electrodes, providing innovative designs for solid-state micro supercapacitors [61]. This integration leverages the conductivity of MXene and the structural stability of carbon black, resulting in synergistic performance improvements.

Similarly, the functionalization of 3D-printed electrodes with MXene for electrochemical capacitors highlights ability of MXene to enhance electrochemical interfaces and conductivity in printed electrodes, offering a promising direction for advanced energy storage devices [62]. Collectively, these advancements emphasize the critical role of MXene in enhancing the properties of conductive materials and smart composites, through cutting-edge 3D printing techniques.

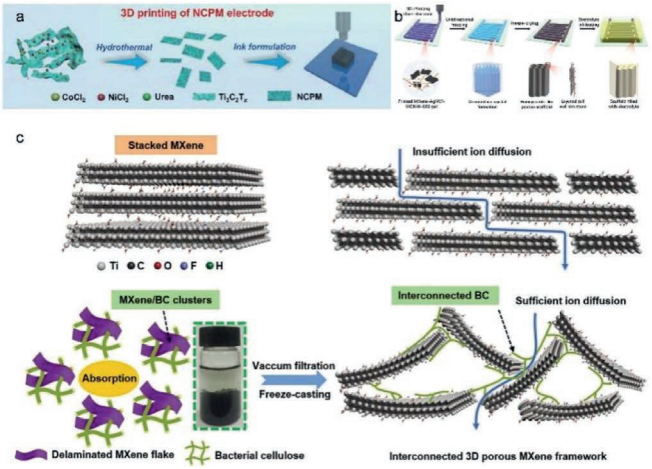


Fig. 8. 3D Printed MXene-based composites for enhanced energy storage and flexible supercapacitor design. (a) 3D printing of NiCoP/Ti_3C_2 MXene architectures for energy storage devices with high areal and volumetric energy density. Reprinted with permission [63]. Copyright 2020, Spinger. (b) Schematic illustration of the fabrication process of intrinsically stretchable MSCs through 3D printing and unidirectional freezing. Reprinted with permission [64]. Copyright 2020, Wiley-VCH. (c) Schematic illustration of the scheme design of porous MXene ($Ti_3C_2T_x$) architecture BC for enhanced electron and ion transport pathways. Reprinted with permission [67]. Copyright 2019, Wiley-VCH.

2.4. Hybrid MXene composites: Merging functional materials for multifunctionality

The development of MXene based composites has led to innovative materials with a wide range of functionalities. For example, NiCoP/Ti_3C_2 architectures and MXene ink containing amphiphilic surfactants, has demonstrated significant potential for printing micro-supercapacitors (MSCs) with high energy density (Fig. 8a) [63]. These advancements highlight the ability of MXene to be combined with other materials to enhance its properties, enabling the design of unique materials that meet the specific requirements of different applications.

One of the most exciting developments involves the fabrication of a pseudoplastic nanocomposite gel using a straightforward 3D printing technique combined with unidirectional freezing. This gel consists of $Ti_3C_2T_x$ MXene nanosheets, manganese dioxide nanowires, silver nanowires, and fullerenes, and is used to create stretchable MSCs with a honeycomb-like porous and staggered electrode structure (Fig. 8b) [64]. The unique architecture of this structure benefits from thick electrodes and three-dimensional porous conductive scaffolds, which improve active material loading, increase interfacial areas, and accelerated ion transport.

This study systematically explores the synergistic relationship between material design, ink formulation, structural optimization, and the resulting multifunctional performance [65]. The 3D-printed chitosan/$Ti_2C_2T_x$-MXene aerogel exhibits an ultralight, porous architecture. By adjusting the MXene content (1, 2, 5, and 10 wt%), the electrical conductivity of the aerogel can be effectively tuned. Additionally, the interaction between chitosan and MXene molecules expands the interlayer spacing of MXene, thereby enhancing the material's structural stability. Furthermore, rheological analysis demonstrates that the incorporation of MXene significantly improves the shear-thinning behavior of the ink, facilitating the 3D printing process. Leveraging digital light processing (DLP) 3D printing technology, an MXene/polyacrylamide hydrogel was successfully fabricated. The introduction of MXene nanosheets not only enhances the hydrogel's wave absorption and mechanical properties but also optimizes the ink formulation,

improves print quality, and enables the fabrication of intricate geometric structures with high precision [66].

These features collectively result in a significant improvement in both energy density and power density, making these MSCs promising for high-performance energy storage devices. Additionally, the fullerene-induced slip cell wall structure contributes to the mechanical robustness of the scaffolds, allowing them to endure significant deformation without fracturing or losing performance. Similarly, the inclusion of biocellulose (BC), provides a highly interconnected nanofiber network with excellent water retention, tensile strength, and rapid ion transport (Fig. 8c) [67]. The self-assembly of MXene nanosheets within the BC network results in a dual-continuous, three-dimensional porous MXene electrode that offers exceptional electron and ion transport pathways, further enhancing the functionality of the composite material.

The integration of MXene with conductive polymer through direct ink writing 3D printing technology has led to the fabrication of programmable MSCs, demonstrating potential of MXene for developing flexible materials [32]. Additionally, the ability to incorporate MXene into flexible substrates through 3D printing techniques has led to the creation of stretchable MSCs, showcasing compatibility of MXene with advanced fabrication methods for flexible electronics [64]. This highlights the versatility of MXene in designing components for stretchable devices, with promising applications in wearable technology. Furthermore, the engineering of 3D ion transport channels within flexible MXene films has been shown to improve both structural integrity and adaptability, illustrating potential of MXene for use in flexible and robust next-generation electronic devices [67]. These developments fully demonstrate the transformative impact of MXene in advancing flexible materials through innovative 3D printing and materials engineering strategies.

In summary, MXene-based composites are revolutionizing 3D printing across a wide range of applications, from biomedical to structural and functional materials. By combining MXene with other materials, its properties are significantly enhanced, demonstrating its vast potential in creating multifunctional materials for a variety of fields. These advancements emphasize the importance of MXene in developing high-performance, flexible, and programmable materials for future technologies.

2.5. Ion doping in MXene: Tailoring electronic properties for advanced applications

MXene materials have attracted significant attention in 3D printing due to their versatility and potential for enhancement through ion doping. Ion doping involves incorporating specific ions into the MXene structure, which can significantly modify its electronic, mechanical, and chemical properties. This process is an effective method for tailoring MXene materials for a variety of applications, from energy storage devices to biosensors and beyond. This section explores recent advancements in ion-doped MXene materials, highlighting how ion doping enhances the functionality of MXene-based structures.

A notable advancement in MXene ion doping is the development of nitrogen-doped $Ti_3C_2T_x$ MXene scaffolds through 3D printing, demonstrating the potential of ion doping for creating porous structures with enhanced properties (Fig. 9a) [68]. Nitrogen doping significantly modifies the electronic characteristics of MXene, leading to improved interactions within the scaffold, which are crucial for optimizing material performance. This strategy highlights the potential of nitrogen-doped MXene in developing advanced materials with promising applications, from energy storage to sensing technologies.

Further advancing ion doping techniques, researchers have explored the use of divalent cation-doped MXene inks in 3D printing applications. Specifically, Ti_3C_2 MXene ink gelated with divalent cations has been utilized in the development of 3D-printed Zn-ion hybrid capacitors. This study highlights the versatility of divalent cation doping in stabilizing MXene inks, thereby enhancing their adaptability in 3D printing processes (Fig. 9b) [69]. The approach demonstrates how divalent cations can significantly enhance the physical and chemical interactions within MXene-based materials, making them more adaptable and stable during the 3D printing process. The findings highlight the versatility of divalent cation doping and its potential to pave the way for new pathways in advanced 3D-printed structures.

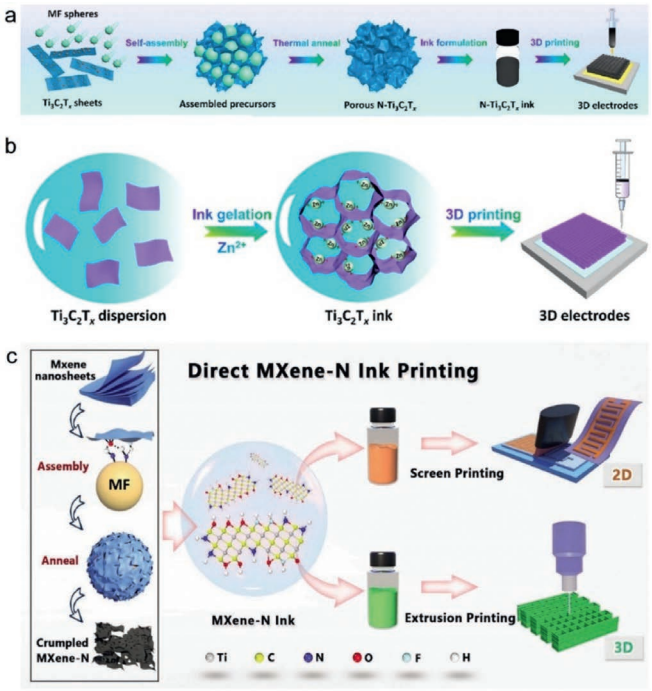


Fig. 9. Ion doping strategies for enhancing the performance of MXene-based structures. (a) Schematic diagram showing the preparation process of 3D-printed electrodes with porous N-$Ti_3C_2T_x$ from MF sphere template. Reprinted with permission [68]. Copyright 2020, American Chemical Society. (b) Schematic diagram showing the preparation of divalent-iongelated MXene ink and 3DP MXene electrodes. Reprinted with permission [69]. Copyright 2021, American Chemical Society. (c) Schematic illustration of direct MXene-N ink printing. Reprinted with permission [70]. Copyright 2019, Wiley-VCH.

Expanding on the nitrogen doping approach, a versatile nitrogen-doped MXene ink has been developed for electrochemical energy storage applications (Fig. 9c) [70]. This ink benefits from the incorporation of nitrogen into the MXene structure, which improves both the printability and functionality of the material. The development of such inks highlights the transformative potential of nitrogen doping in enhancing the versatility of MXene inks, enabling the creation of complex and functional 3D-printed materials with improved electrochemical performance. This innovation is a step forward in the design of advanced materials for energy storage applications, demonstrating adaptability of MXene for various technological uses.

The studies presented in this section emphasize the transformative role of ion doping in advancing MXene-based 3D printing applications. By employing different ion-doping strategies, researchers have successfully expanded the scope and utility of MXene materials, paving the way for innovative designs and functional materials across various fields. Moreover, these advancements demonstrate the growing synergy between material science and 3D printing technology, establishing MXene as a key material for the future of advanced manufacturing and materials

development. Ion doping, with its ability to tailor material properties, holds great promise for enhancing the performance and applicability of MXene in next-generation technologies.

In summary, MXene-based materials exhibit great promise for energy storage applications, particularly when integrated with 3D printing technologies. These insights set the stage for exploring the complementary advantages of MOF-based systems.

2.6. Rheomechanical mechanisms of MXene-based materials in 3D printing

2.6.1. Interaction mechanisms between components

The synergistic interactions between MXene and nanofillers rely on electrostatic interactions, hydrogen bonding, van der Waals forces, surfactant modulation, and ionic crosslinking mechanisms to optimize the rheological properties and structural stability of inks. The negatively charged functional groups (-O, -OH) on MXene surfaces (*e.g.*, $Ti_3C_2T_x$) form dynamic crosslinked networks with cationic additives (*e.g.*, Zn^{2+}, Ca^{2+}) *via* electrostatic attraction, significantly enhancing the yield stress (τ_n) and storage modulus (G'). For instance, MXene-Zn-0.03 ink with 0.03 mg/mL Zn^{2+} exhibits a G' of 3×10^3 Pa and τ_n of 100 Pa [69]. Additionally, MXene interacts with cellulose nanofibers (CNF) or graphene oxide (GO) through hydrogen bonding and van der Waals forces to form stable 3D networks, improving thixotropic recovery (*e.g.*, >99 % viscosity recovery for MXene/CNF10 ink) [52].

Furthermore, divalent cations (Zn^{2+}, Ca^{2+}) shield the negative charges on MXene surfaces, promoting nanosheet crosslinking to form porous gel structures (verified by XRD, showing reduced interlayer spacing with increasing Zn^{2+} concentration) [69]. However, excessive cations (*e.g.*, Zn^{2+} > 0.05 mg/mL) may induce aggregation dominated by van der Waals forces, compromising ink homogeneity. Thus, rational regulation of MXene-filler interactions is critical for high-performance inks.

2.6.2. Correlation between rheological properties of MXene inks and 3D printing performance

The rheological properties of MXene inks are intrinsically linked to 3D printing performance, with shear-thinning behavior, yield stress modulation, viscoelastic matching, and thixotropic recovery being key factors for print quality optimization. At high shear rates (>100 s^{-1}), the rupture of physical connections between MXene nanosheets leads to rapid viscosity reduction (*e.g.*, MXene-Fe/SiC ink viscosity drops from 10^5 Pa s to 10^2 Pa s), enabling smooth extrusion [58]. A lower shear-thinning index (n) enhances shear sensitivity; for example, ink with $n = 0.73$ achieves high-resolution printing (≈165 μm line width) through a 290 μm nozzle [63].

Yield stress (τ_n) critically influences interlayer adhesion. Low τ_n (< 100 Pa) may cause gravitational collapse and excessive layer fusion (*e.g.*, MXene-Zn-0.01 ink fails to form self-supporting structures), while high τ_n (> 200 Pa) suppresses collapse but requires optimized printing pressure (*e.g.*, MXene/CNF10 ink with $\tau_n = 191.56$ Pa supports 10-layer stacking without deformation under 28 kPa) [52,69]. Viscoelastic matching ensures shape fidelity: Elastically dominated inks ($G' > G''$) exhibit solid-like behavior (*e.g.*, MXene/C12E9 ink: $G' = 2.05 \times 10^5$ Pa, $G'' = 6.01 \times 10^4$ Pa), whereas viscous dominance ($G'' > G'$) in high-shear regions (*e.g.*, nozzle interior) facilitates extrusion [32,71]. 52 Thixotropic recovery is vital for multilayer printing. MXene/CNF10 ink achieves > 99 % viscosity recovery within 10 s post-shear, enabling complex architectures (*e.g.*, grids, cantilevers), whereas pristine MXene ink requires CNF or MWCNT additives to enhance network stability [52,53]. Therefore, rational rheological parameter control enhances printing precision and structural stability.

2.6.3. Influencing factors on print quality

Print resolution of MXene inks is governed by nozzle diameter, printing speed, and interlayer adhesion strength, while long-term stability is critical for structural integrity. A 400 μm nozzle combined with ink exhibiting a shear-thinning index of $n = 0.71$ achieves a line width of ≈200 μm [64]. Increasing printing speed reduces line width; for example, raising speed from 2 mm/s to 5 mm/s decreases line width from 355 μm to 165 μm [63]. For interlayer adhesion, viscoelastic matching is essential: A storage modulus (G') slightly exceeding the loss modulus (G'') ($\tan\delta \approx 0.5$–1.0) ensures robust layer fusion without collapse [43].

Long-term stability requires environmental control. MXene/C12E9 ink maintains structural integrity for over 1 h under static conditions, supporting complex architectures, whereas Zn^{2+}-containing inks must avoid humidity fluctuations to prevent gel dehydration and performance degradation [69,71]. By optimizing rheological parameters, printing protocols, and environmental conditions, MXene-based 3D printing can achieve enhanced resolution, interlayer stability, and long-term durability.

3. Applications of MOF-based functional materials in 3D printing

The integration of MOFs and gel materials in 3D printing has significantly advanced ink formulation strategies, resulting in enhanced printing quality, mechanical stability, and functional performance of printed materials [72–76]. MOFs, known for their high specific surface area and tunable porosity, offer unique benefits for optimizing ink properties by modulating printability, mechanical strength, and functionality. Gel materials, recognized for their excellent biocompatibility, tunable rheology, and environmental adaptability, further improve ink formulations by enhancing stability and facilitating the integration of active materials into printable systems [77–84]. This section provides the diverse applications of MOFs and gel materials in 3D printing inks, examining the underlying mechanisms that drive their effectiveness and summarizing strategies highlighted in the literature. Specific attention is given to how these materials contribute to functional enhancements in various fields, illustrating how modifications in ink properties translate to improved real-world performance.

3.1. MOF-polymer gels for enhanced ink performance

3.1.1. Tailoring 3D printing inks with MOF modulation

The unique porous structure and tunable surface chemistry of MOFs provide a powerful approach for enhancing 3D printing ink properties. For example, the *in-situ* growth of MOFs within hydrogels can effectively modulate the mechanical and rheological properties of inks [85]. By tailoring the synthesis conditions of MOFs, factors such as particle dispersion, mechanical strength, and structural stability within hydrogels can be precisely controlled, thereby optimizing the rheological behavior of inks for 3D printing. Additionally, the gas storage capabilities of acrylonitrile butadiene (ABS)-MOF composite have revealed the potential of MOFs to enhance gas adsorption within inks, making them particularly valuable for applications in gas sensing and environmental monitoring [86]. These findings illustrate the versatility of MOFs in enhancing both the functionality and mechanical performance of 3D-printed materials.

In MOF-polymer composites, the incorporation of MOFs into methacrylated gelatin scaffolds has been shown to significantly enhance mechanical stability, and structural integrity, leading to improved print quality and resolution [87]. Similarly in biomedical applications, MOF-doped bio-printable hydrogels have demonstrated promising potential for bone repair, where improved print

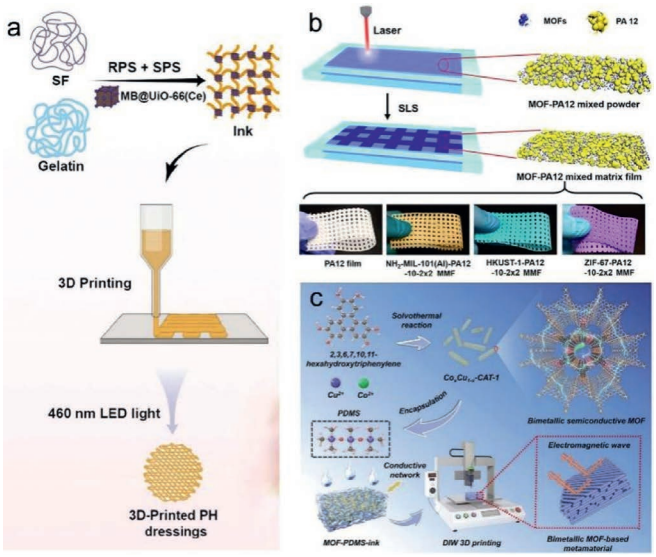


Fig. 10. Design strategies and fabrication processes of MOF-based 3D printing inks. (a) Schematic representation of the design strategy for MOF-based 3D printing inks. Reprinted with permission [91]. Copyright 2023, The Author(s). (b) Schematic procedure for printing MOF-PA12 mixed matrix films (MMFs) with grid patterns and along with photographs of the PA12 film and MOF-PA12 MMFs incorporating various MOF fillers. Reprinted with permission [97]. Copyright 2019, American Chemical Society. (c) Schematic illustration of the preparation process for bimetallic SC−MOF metamaterial absorbers highlighting the integration of MOFs with gel materials for enhanced electromagnetic shielding. Reprinted with permission [98]. Copyright 2024, Wiley-VCH.

performance and mechanical properties are essential [88]. The reinforcing role of MOFs in polymer matrices illustrates their critical contribution to advancing 3D-printed biomaterials, opening avenues for further development in fields such as tissue engineering and regenerative medicine.

3.1.2. Role of gel materials in ink optimization

Gel materials, including gelatin and alginate, are widely employed in 3D printing due to their exceptional biocompatibility and customizable properties. By adjusting the composition and cross-linking density of these gels, such as alginate/gelatin scaffolds integrated with ZIF-8, researchers have shown substantial improvements in the rheological properties and printing precision of inks. For example, controlling cross-linking density optimizes flow behavior, which is critical for consistent and accurate printing [89]. Additionally, MOF nanoenzyme hydrogels demonstrate dual enzymatic activities that enhance multifunctionality in applications like glucose monitoring, showcasing the potential of functionalized gels [90]. Moreover, studies with silk fibroin and gelatin hydrogels crosslinked with MOF-methylene blue nanoparticles, reveal enhancements in mechanical properties and bioactivity, promoting high performance in biological applications where biological compatibility is essential (Fig. 10a) [91].

Integrating MOFs with gel matrices yields synergistic improvements in both functional and structural properties of 3D printing inks. For example, MOF-based ionogels exhibit enhanced colorimetric and mechanical characteristics, which contribute to improved print stability and aesthetic qualities in printed materials [92]. Additionally, incorporating photocurable resins with MOFs for micro-optofluidic applications has shown significant gains in optical and mechanical performance, underscoring the versatility of gel-based inks across diverse fields [93]. By selecting polylactic acid (PLA) as the matrix and incorporating highly porous HKUST-1 MOF, the composite material is endowed with enhanced adsorption functionality [94]. To improve flexibility and lower the glass transition temperature (T_g), polyethylene glycol dimethyl ether (PEGDME) is employed as a plasticizer, ensuring that the material maintains excellent printability even with a 50% MOF loading. Furthermore, to achieve a homogeneous slurry, solvent dispersion and ball milling processes are utilized, promoting the uniform distribution of MOF particles and preventing brittle fractures caused by particle agglomeration. In combination with the optimization of extrusion process parameters, uniform 3D-printed filaments are successfully fabricated. At the microstructural level, MOF particles form a continuous network within the composite, preserving a high specific surface area and an accessible adsorption window. Overall, the successful 3D printing of long filaments with high MOF loading overcomes the limitations of traditional loading methods, streamlining the fabrication process and expanding the potential for functional applications such as water treatment and gas capture. This work exemplifies an advanced material design strategy based on the synergistic optimization of composition, structure, and performance.

Additionally, Idrees *et al.* [95] leveraged 3D printing technology to construct a novel grid-reservoir-integrated anode using a UiO-66-NH_2 MOF precursor. Through the coordination and pyrolysis of polydimethylsiloxane (PSO), a mesoporous carbon (MPC)-silicon oxycarbide (SiOC) interpenetrating network was formed. The MPC component provides high conductivity and a large specific surface area, while SiOC enhances mechanical stability and optimizes zinc nucleation behavior. Furthermore, the combination of MPC, SiOC, and PVDF forms a shear-thinning gel, optimizing the ink's rheological properties and ensuring structural integrity after 3D printing. The resulting well-defined grid structure effectively enhances Zn^{2+} storage capacity and mitigates dendrite formation, demonstrating the potential of 3D-printed architectures for next-generation energy storage systems. These advancements emphasize the versatility of gel materials in optimizing ink performance for applications ranging from biomedical devices to optoelectronic systems.

3.1.3. Challenges and mechanisms in MOF-gel ink development

The integration of MOFs and gel materials into 3D printing inks offers several key advantages, particularly in modulating rheological properties, drying rates, and mechanical performance. For example, research on high-porosity filters fabricated with MOF composites through selective laser sintering has shown how MOFs can significantly influence the printing process by enhancing the porosity and structural integrity of the printed materials [96]. Similarly, studies on MOF-based mixed matrix films for water treatment illustrate the versatility of MOFs in adjusting ink properties to suit specific functional needs (Fig. 10b) [97]. The synergistic effects of combining MOFs with gel materials are also of significant interest, as this pairing can further enhance the performance of printable inks. For example, the development of multi-scale MOF metamaterials for broadband microwave absorption highlights how the precise integration of MOFs with gel can result in advanced functionalities, such as improved electromagnetic shielding (Fig. 10c) [98].

Moreover, the use of MOF mixed-matrix coatings in 3D-printed devices has demonstrated substantial improvements in coating performance, especially when combined with gel materials [99]. This combination enhances the material's durability, adhesion, and overall mechanical properties, making it ideal for high-performance, complex 3D-printed structures. Additionally, research on ABS-MOF composites for hydrogen storage has demonstrated that MOFs can be engineered to create inks with tailored storage capacities, emphasizing the crucial role of MOFs in improving the functional properties of 3D-printed materials [100].

Despite the significant potential of MOFs and gel materials in modulating printable inks, several challenges remain. One of the primary obstacles is the efficient dispersion and stability of MOFs

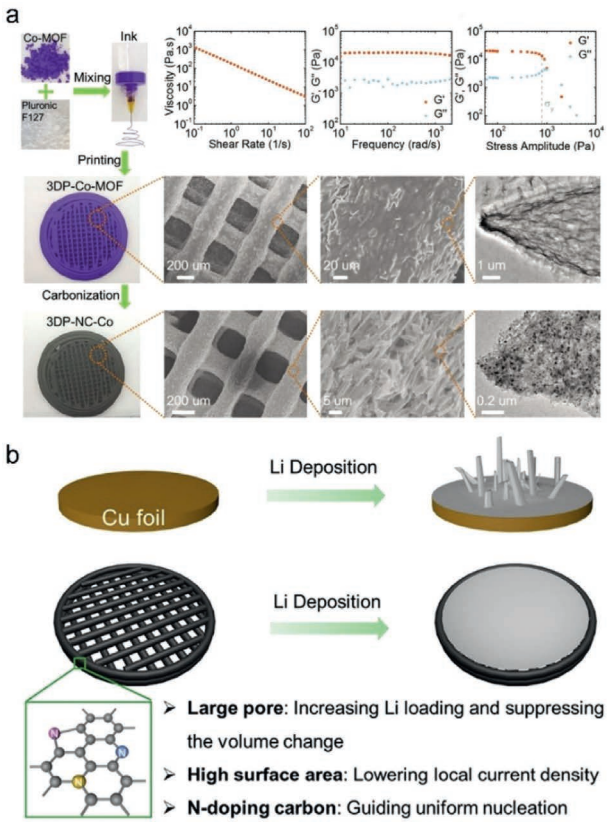


Fig. 11. Enhanced rheological and electrochemical performance of MOF-derived frameworks. (a) Preparation and characterization of 3D-printed Co-MOF-derived hierarchical framework, highlighting its influence on ink rheology and flow characteristics for enhanced printability and electrochemical performance. Reprinted with permission [102]. Copyright 2018, Wiley-VCH. (b) Schematic illustration of the lithium plating process, showing how the structural properties of MOF-derived frameworks impact electrode porosity, conductivity, and battery performance during Li–O_2 and lithium metal battery operation. Reprinted with permission [103]. Copyright 2019, Elsevier.

within the ink matrix, which is crucial for achieving uniformity in the printed structure. Additionally, controlling the cross-linking of gels is vital for maintaining the desired rheological properties and mechanical performance during and after printing. Future research should focus on optimizing the synthesis and dispersion techniques of MOFs to ensure more stable, homogeneous mixtures, and develop advanced cross-linking strategies for gel materials to improve the overall printing process.

3.2. MOF derivatives for high-performance 3D printing

The integration of MOF derivatives into printable inks has revolutionized 3D printing by offering enhanced control over ink properties and print quality [101]. MOF-derived materials, with their unique structural characteristics and versatile functionality, play a pivotal role in fine-tuning the rheological and mechanical properties of inks. This section reviews recent advancements in the use of MOF-derived materials for tuning printable inks, highlighting their influence on ink formulation strategies and overall print performance.

MOF-derived materials provide considerable advantages in modulating the rheological properties of printable inks. One prominent example is the integration of MOF-derived, hierarchically porous frameworks into inks, which has shown a profound ability to influence flow characteristics and ink stability (Fig. 11a) [102]. For instance, MOF-derived porous frameworks have been crucial in enhancing the printability and electrochemical performance for high-energy density Li–O_2 and lithium metal batteries. The hierarchical porosity of these frameworks allows for precise control over ink viscosity and flow behavior, ensuring structural stability while optimizing electrochemical performance. By controlling the distribution and viscosity of MOF particles within the ink, formulations can be tailored to modulate electrode porosity and conductivity, and ultimately, battery performance. Careful regulation of rheology, including viscosity, and dispersion is crucial for adapting to diverse printing processes and meeting the specific requirements of electrodes (Fig. 11b) [103]. By tailoring the MOF structure, the dispersion and interaction of MOF particles within the ink matrix can be manipulated. This adjustment directly impacts both print quality and the functionality of the final product, showcasing the flexibility of MOFs in a variety of 3D printing applications.

MOF derivatives also play a crucial role in enhancing the mechanical properties of 3D-printed structures. One example is the use of MOF-based Boehmite inks for producing Fe/γ-Al_2O_3 monoliths [104]. The study demonstrated that the inclusion of MOF-derived materials improves the structural integrity and mechanical strength of printed objects. The inclusion of MOF-derived materials enhances the ability of inks to form robust and durable prints, which is essential for applications requiring high mechanical stability.

Similarly, the development of porous magnetic carbon materials derived from MOFs further highlights the impact of these materials on the mechanical properties of printed structures [105]. The incorporation of MOF-derived magnetic carbon into the ink matrices enhances enhance the mechanical performance and dimensional stability of the printed objects, making them more suitable for demanding applications.

The functionalization of MOF derivatives offers significant advantages in tailoring ink properties for specific applications. For instance, ZIF-8 has been employed in the development of near-infrared light-responsive biosensors, demonstrating how MOF derivatives can be fine-tuned to enhance their responsiveness to external stimuli, thereby increasing the versatility of printable inks [106]. Additionally, the integration of MOF-derived microporous Mn_2O_3-modified electrodes in microfluidic devices has been shown to significantly enhance functionality, including real-time detection capabilities [107]. The increased surface area and controlled porosity of these MOF materials facilitate rapid analyte interaction, leading to improved detection sensitivity and performance. This adaptability emphasizes the potential of MOF derivatives to expand the range and capabilities of printable ink, enabling a variety of advanced applications.

Despite these advancements, several challenges remain in optimizing MOF-derived materials for ink modulation. Key issues include achieving uniform dispersion of MOFs within inks, ensuring the stability of these particles during the printing process, and understanding their interactions with other ink components. Addressing these challenges will require ongoing research focused on refining the synthesis and integration of MOF derivatives into printable inks. Future studies should focus on developing novel MOF structures with tailored properties that address specific printing requirements. Additionally, a deeper understanding of how MOFs interact within the ink matrix will be critical for achieving more effective control over ink behavior and improve overall print quality. Advancements in sustainable MOF synthesis methods and the development of hybrid materials with customizable properties for broader applications will further enhance the potential of MOF derivatives in 3D printing.

In summary, MOFs derivatives provide a powerful tool for modulating the rheological, mechanical, and functional properties of printable inks. By strategically manipulating the structure of MOFs and incorporating them into inks, researchers can achieve superior

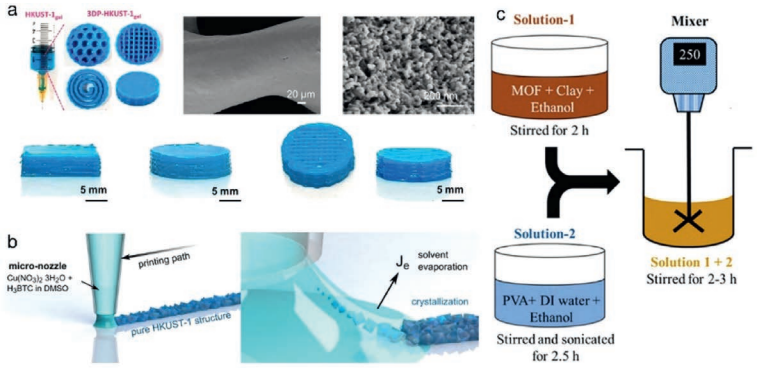


Fig. 12. Optimizing 3D printing of MOF structures: Ink formulation, precision printing, and preparation process. (a) HKUST-1gel loaded into a syringe showing different 3D printed structures formed from the MOF ink. Reprinted with permission [108]. Copyright 2019, American Chemical Society. (b) 3D printing of a pure metal–organic framework, showing the effect of nozzle diameter on print resolution and structural integrity. Reprinted with permission [110]. Copyright 2022, American Chemical Society. (c) Schematic illustration of the 3D-printed MOF monolith preparation procedure, highlighting the steps involved in ink formulation and printing optimization. Reprinted with permission [109]. Copyright 2017, American Chemical Society.

print quality, functionality and performance. Continued research in this area promises further advancements in 3D printing technology, driven by the innovative application of MOF derivatives.

3.3. Pure MOF: Structural integrity in additive manufacturing

The application of pure MOF materials in 3D printing has seen significant advancements, driven by strategies to optimize ink formulations and printing techniques. These optimizations are essential for achieving superior printing outcomes, ensuring high-quality printed structures with enhanced functionality.

Effective incorporation of MOF materials into 3D printing inks requires the precise formulation of inks to ensure stable and consistent printing. A key strategy involves refining the solvent and surfactant compositions to improve the dispersion of MOF particles and prevent particle agglomeration., This approach ensures uniformity and integrity throughout the printing process (Fig. 12a) [108]. By preventing particle agglomeration, the ink maintains consistent flow and ensures the printed structure's quality and stability. Moreover, adapting ink viscosity is critical for accommodating various printing techniques. The viscosity is adjusted by varying the concentration of binders, ensuring the ink is compatible with both inkjet and extrusion-based printing methods (Fig. 12c) [109]. This flexibility allows for tailored ink formulations that are optimized for diverse printing approaches, enabling precision and high-resolution printing.

Equally important is the optimization of printing parameters, which directly influence the precision and quality of 3D-printed MOF-based constructs. Adjustments to printing parameters, such as nozzle diameter, printing speed, and interlayer adhesion, are essential for achieving the desired structural integrity, particularly for microstructures. The precise control of these parameters ensures that the final print meets the required specifications in terms of resolution and strength (Fig. 12b) [110]. Additionally, the incorporation of support materials plays a key role in preventing deformation during the printing process, especially when printing complex geometries. These supports maintain the structural stability of MOF monoliths, which are often prone to distortion due to the material's inherent properties [111].

The selection and modification of ink types are critical to achieving successful 3D printing outcomes. Aqueous inks, with their lower viscosity, are well-suited for inkjet printing, where fine details and high resolution are required. In contrast, organic solvent-based inks are more appropriate for extrusion printing as their higher viscosity allows for the formation of more robust and stable structures [112]. Additionally, chemical modifications to the ink are essential for enhancing the adhesion between MOF particles and printing substrates. These modifications enhance the overall print quality by improving the bonding strength and structural stability of the printed materials, ensuring durability in the final structures [113].

In summary, significant progress has been made in applying pure MOF materials in 3D printing. Key strategies include optimizing ink formulations, adjusting printing methods, and selecting the appropriate ink types. These optimization strategies ensure the effective utilization of MOF materials into the printing process, enhancing the quality, precision, and durability of the printed structures. By refining these strategies, the full potential of MOFs can be realized in 3D printing applications, unlocking new possibilities for advanced material design and functional devices.

3.4. MOF composites: Revolutionizing hierarchical and functional structures

The integration of MOF composites into 3D printing inks and techniques has become a focal point for advancing material performance and structural design in additive manufacturing [114–117]. The following section reviews the application of MOF composites in 3D printing, detailing various strategies for ink modulation, types of composites used, and printing techniques to optimize functional outcomes.

The development of hierarchical structures using MOF-based composites has significantly enhanced the performance and printable inks [111]. One notable approach is the combination of MOFs with clay to create 3D-printed hierarchical porous architectures (Fig. 13a). This integration improves the dispersion and stability of MOF particles within the ink, preventing particle aggregation and ensuring a consistent flow during printing process. By fine-tuning the rheological properties of the ink, challenges such as MOF particle aggregation are effectively addressed, leading to uniformly printed structures that maintain structural integrity. Similarly, the formulation of an Al-based MOF/S cathode composite ink highlights the importance of controlling ink viscosity and achieving homogeneous particle distribution (Fig. 13b) [112]. These adjustments are crucial for maintaining the stability of the printed cathodes, ensuring high-quality prints even for complex 3D structures. These findings emphasize how the optimization of ink composition directly impacts the printing outcome, improving both the resolution and mechanical properties of the final product.

The synergistic effects of Ni^{2+}-intercalated cobalt organic frameworks in 3D-printed micro-supercapacitor electrodes highlight the importance of optimizing the interaction between MOF

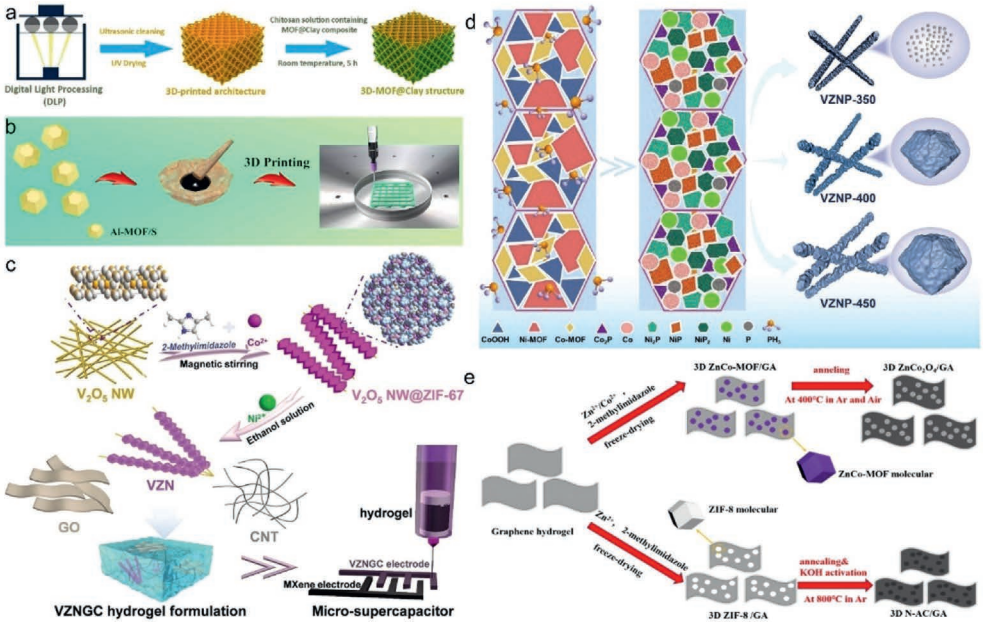


Fig. 13. MOF-based composite ink formulation and 3D printing processes for advanced material structures. (a) Schematic representation of the fabrication of the 3D-MOF@clay composite structure, highlighting the integration of MOF particles with clay to form hierarchical porous architectures. Reprinted with permission [111]. Copyright 2022, The Royal Society of Chemistry. (b) Schematic illustration of the preparation of Al-based MOF/S composite ink and the 3D printing process, emphasizing the importance of controlling ink viscosity and particle distribution for high-quality prints. Reprinted with permission [112]. Copyright 2023, The Royal Society of Chemistry. (c) Schematic illustration of the preparation of VZN composite ink for 3D printed micro-supercapacitor, focusing on the optimization of ink composition to improve structural stability and conductivity. Reprinted with permission [118]. Copyright 2023, Wiley-VCH. (d) Schematic diagram depicting the controllable adjustment of material morphology by increasing the variety of phosphides through multivalent nickel metal doping under nitrogen protection atmosphere, enhancing material performance in energy storage devices. Reprinted with permission [119]. Copyright 2024, Wiley-VCH. (e) Schematic diagram illustrating the formulation of a 3D-printed composite ink based on MOFs derived active material and graphene aerogels, highlighting the balance of viscosity, dispersion, and printability. Reprinted with permission [120]. Copyright 2022, Elsevier.

particles and conductive polymers within the ink (Figs. 13c and d) [118,119]. By adjusting the ink composition, both the electrical conductivity and structural stability of the printed electrodes are significantly improved. These advancements emphasize the critical role of ink formulation in creating high-performance 3D-printed devices, particularly in energy storage applications.

Recent developments in composite inks incorporating MOFs alongside materials such as graphene aerogels and cellulose have significantly expanded the potential for 3D printing for a variety of applications (Fig. 13e) [120]. The rational design of these composite inks is crucial for ensuring printability and functionality. For example, combining MOF-derived active materials with graphene aerogels has proven effective in applications like alkaline battery-supercapacitor hybrid devices. Achieving the optimal balance of viscosity, dispersion, and printability through careful selection and modification of ink components is essential for the success of these applications.

Another promising innovation is the development of sustainable composite inks using cellulose and zeolitic imidazolate frameworks (ZIFs). These inks enable the 3D printing of structures with functional properties such as CO_2 and heavy metal ion adsorption (Fig. 14a) [121]. The careful choice of binders and solvents plays a vital role in optimizing rheological properties, ensuring high-resolution and precise printing of complex structures. This innovation highlights the importance of tailoring ink formulations to meet specific performance requirements in advanced 3D printing applications.

In summary, the modulation of printable inks using MOF composites is a multifaceted process that requires careful consideration of various factors including particle dispersion, viscosity, rheological properties, and the interaction between MOFs and other ink components. The studies reviewed in this section demonstrate the versatility of MOF-based composite inks in overcoming challenges related to 3D printing, paving the way for the development of advanced materials with tailored properties. By strategically optimizing ink formulations, researchers have successfully integrated MOF composites into a wide range of 3D-printed structures, showcasing the potential of these materials in the ever-evolving field of additive manufacturing.

3.5. 3D printing templates for MOF integration

These templates not only serve as the structural foundation for printing but also significantly influence the functionality and performance of the final printed material. This section outlines the key methods for fabricating MOF-based templates including spraying, dripping, casting, *in-situ* growth, and hybrid integration, highlighting their role in enhancing the properties of printed materials.

3.5.1. MOF spraying techniques for controlled deposition

MOF spraying techniques are pivotal in applying MOF materials onto substrates or integrating them into 3D-printed structures, typically resulting in thin films or coatings [122–124]. This approach is particularly useful for creating mixed matrix thin-film membranes, where MOFs are uniformly distributed within a polymer matrix, leading to enhanced properties. The use of spray coating methods also facilitates the integration of functionalized MOFs onto 3D-printed devices, optimizing the interaction between the coating and the structure to enhance overall device performance (Fig. 14b) [125].

Spraying techniques offer great versatility, enabling the deposition of MOFs onto complex 3D-printed constructs with tailored functionalities. This adaptability allows for the development of MOF-functionalized structures that can enhance properties like conductivity, catalytic activity, and mechanical stability for a wide range of applications. The precision of spray-based deposition,

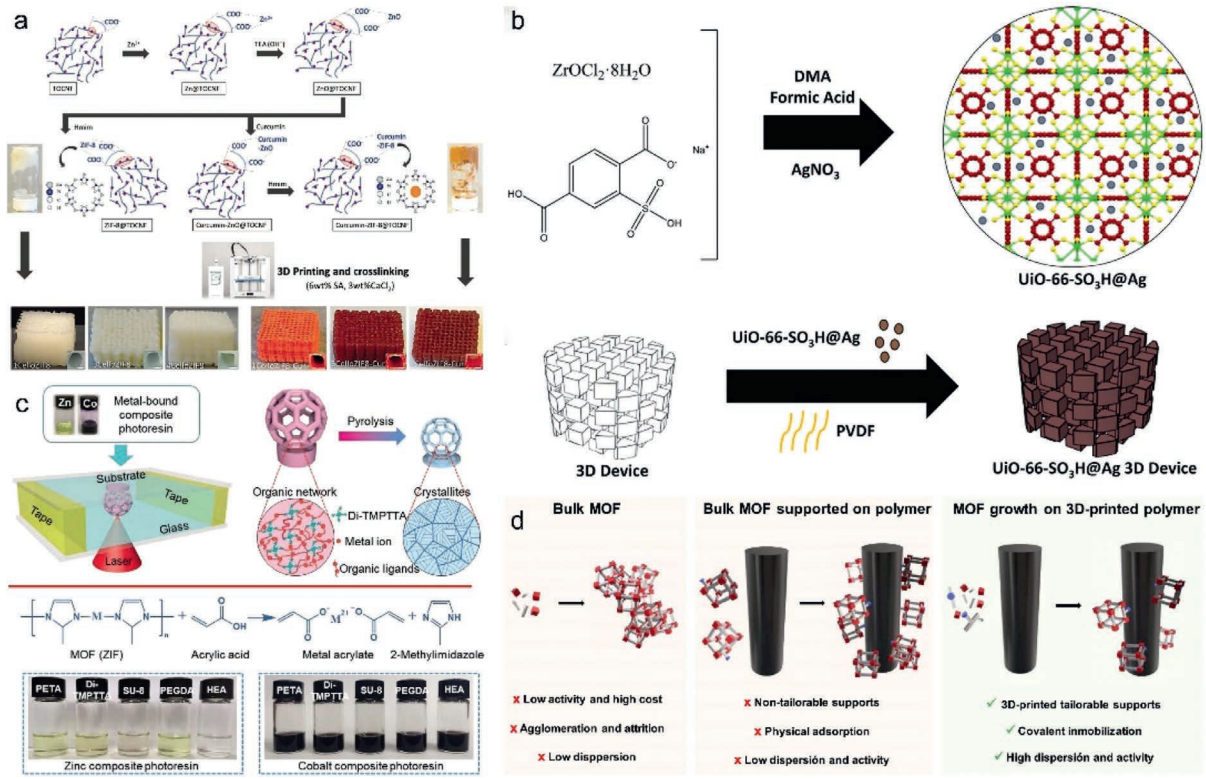


Fig. 14. Advancements in MOF-based 3D printing: Techniques, inks, and functional applications. (a) Schematic representation of the synthesis and 3D printing of cellulose-ZIF8 hybrid inks with and without curcumin, showcasing their potential for functional material design. Reprinted with permission [121]. Copyright 2018, Wiley-VCH. (b) Schematic representation of the preparation, process for integrating MOFs into 3D-printed structures, emphasizing their role in enhancing performance. Reprinted with permission [125]. Copyright 2021, Elsevier. (c) Manufacturing route for 3D nano-architected metal oxide semiconductors, using MOF-based composite inks, highlighting the precision of the process. Reprinted with permission [127]. Copyright 2021, Wiley-VCH. (d) Overview of state-of-art MOF technologies, comparing the use of bulk powder (left) and post-synthetic adsorption of MOFs on polymer surfaces (center), one-pot growth of MOF on 3D-printed materials with functional groups for the covalent immobilization of the MOF (right), illustrating the versatility in MOF integration techniques for advanced materials. Reprinted with permission [140]. Copyright 2023, Elsevier.

along with the ability to control thickness and uniformity, positions this technique as an effective strategy for advancing MOF-based functionalization in 3D printing.

3.5.2. Dripping and casting techniques for complex designs

Dripping and casting are liquid-phase processes used to integrate MOF materials into 3D-printed structures, often resulting in complex shapes or enhanced properties [126]. Dripping techniques utilize composite photoresins containing metal-bound MOFs to create nano-architected structures. These structures are then cured into solid matrices, often semiconductor-based providing high precision and intricate detailing (Fig. 14c) [99,127]. This method is particularly useful for incorporating MOFs into specific regions of a structure, enabling the creation of localized functionalities.

Casting techniques, on the other hand, involve embedding MOFs, such as HKUST-1, into 3D-printed metal lattices [128]. This approach requires uniform MOF distribution throughout the lattice structure, ensuring both structural integrity and optimizing functional performance. Additionally, casting techniques have been adapted to synthesize MOF/SiO_2 composites, offering flexibility in tailoring material properties [129]. The flexibility of casting in creating composites with specific attributes highlights its adaptability across various MOF systems and functionalities [127–129].

The complementary nature of dripping and casting techniques offers pathways for integrating MOFs into 3D-printed materials. While dripping excels in the precision of nano-architectures, casting focuses on uniform integration, making it ideal for larger-scale applications that demand structural consistency. Together, these methods provide a versatile toolkit for embedding MOFs into 3D-printed materials.

3.5.3. In-situ growth strategies for advanced MOF applications

In-situ growth techniques enable the direct formation of MOFs on or within 3D-printed substrates, creating structures with seamlessly integrated functionalities [130–138]. A common approach involves solvothermal synthesis, where MOFs framework grows directly within pre-printed structures, enhancing the functionality of the substrate (Fig. 14d). This method results in a well-integrated MOF network that can significantly improve properties such as chemical stability, catalytic activity, and electrical conductivity.

Bauza *et al.* [139] integrated ZIF-8 metal-organic frameworks (MOFs) with 3D printing technology, employing an *in situ* growth method to deposit ZIF-8 onto the surface of a 3D-printed substrate. Subsequently, high-temperature carbonization was utilized to prepare ZIF-8-derived carbon (c-ZIF-8) with a hierarchical microporous-mesoporous structure. This process not only eliminates the Zn component, thereby enhancing the water stability of the material, but also preserves structural integrity through strong interfacial bonding between the MOFs and the substrate. From a material control perspective, the interconnected cubic array structure fabricated *via* 3D printing optimizes the specific surface area, effectively improving the overall performance of the material.

Another promising method is one-pot growth, where MOFs are synthesized directly on polymeric substrates during the 3D printing process. This allows for a seamless incorporation of MOFs into the polymer matrix, reducing processing complexity while maintaining material properties [140]. Additionally, the integration of MOFs within nanocellulose matrices through *in-situ* growth combines the unique properties of both materials, leading to innovative 3D-printed structures with enhanced mechanical strength, porosity, and surface area [121,124,141]. These diverse *in-situ* techniques

demonstrate the flexibility of *in-situ* growth techniques in embedding MOFs into 3D-printed substrates, contributing to the advancement of functional materials with tailored properties.

3.5.4. Hybrid and functionalized MOF templates for multi-functional devices

The strategic combination of MOFs with other materials or their functional modification plays a crucial role in enhancing the properties of 3D-printed structures. One effective approach integrates MOFs into flexible fibers, resulting in high MOF loading while preserving adaptability of materials across diverse applications [76,142–145]. For example, the incorporation of magnetic MOFs into 3D-printed microchips exploits the inherent magnetic properties of MOFs, significantly expanding their utility in analytical applications [145]. Functionalizing MOFs for precise control over their physical, chemical, and mechanical properties, further enhances the potential of 3D printing technologies. This strategy not only improves the overall functionality of the printed structures but also enables the development of materials with customized properties, making them suitable for a wide range of applications from biomedical devices to energy storage systems. By combining MOFs with other materials and modifying their properties, researchers can create 3D-printed devices with enhanced performance, pushing the boundaries of functional material design.

3.6. Innovative approaches in MOFs integration for 3D printing

The integration of MOFs into 3D-printed structures is an evolving area of research that leverages various techniques to enhance the properties and functionalities of advanced materials. This section explores three prominent approaches: The exploration and implementation of ink regulation strategies, the application of MOFs in functionalized structures, and advancements in high-precision 3D printing technologies.

3.6.1. Novel approaches to ink regulation for enhanced MOF integration

The design and regulation of inks are essential to advancing 3D printing technologies, particularly for the fabrication of materials with enhanced functionalities. A breakthrough development in this area involves the creation of a universal room-temperature 3D printing technique for producing porous MOF-based hybrid solid-state electrolytes. This method significantly improves safety and stability by inhibiting dendrite growth in battery systems (Fig. 15a) [146]. The application of MOFs for active ink regulation has also shown promise in ZIBs, where 3D-printed energy storage grids have been successfully incorporated into anodes, achieving dendrite-free growth (Fig. 15b) [147]. These studies emphasize the critical role of ink regulation in improving the functionality and stability of advanced materials used in energy storage devices.

3.6.2. Functionalized MOFs for next-generation structural applications

The structural functionalization of MOFs plays a crucial role in the advancement in the field of 3D printing technologies [116,148,149]. Recent studies have demonstrated the potential of MOFs in enhancing the functional properties of 3D-printed structures. For example, 3D-printed zeolitic imidazolate framework have shown remarkable improvements in adsorptive separation performance, highlighting their potential for applications in gas separation and filtration (Fig. 15c) [150,151]. Similarly, the growth of UTSA-16 MOFs within 3D-printed co-kaolin monoliths has shown high selectivity in CO_2/CH_4, CO_2/N_2, and CO_2/H_2 separations, showcasing the versatility of MOFs in environmental and industrial applications [152–155]. These examples highlight the growing potential of MOFs in creating highly functional 3D-printed materials for a range of applications, from selective adsorption to catalytic processes.

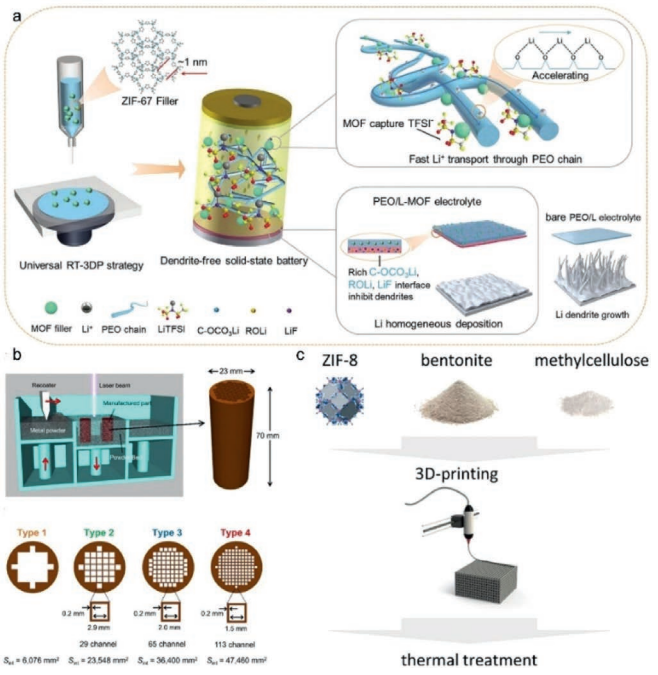


Fig. 15. Innovative strategies for integrating MOFs in 3D printing: Ink regulation, functionalized structures, and precision fabrication. (a) Schematic illustration of the universal room-temperature 3D printing strategy for producing dendrite-free solid-state lithium metal batteries, highlighting the enhancement of safety and stability through the suppression of dendrite growth. Reprinted with permission [146]. Copyright 2023, Wiley-VCH. (b) Schematic representation of the laser powder bed fusion apparatus for the fabrication of Cu-based flow reactors in a cylinder shape, for energy storage applications, showcasing the precision of additive manufacturing in reactor design. Reprinted with permission [147]. Copyright 2023, American Chemical Society. (c) Schematic overview of the synthesis procedure used to create ZIF-8-based 3D-printed structures, where ZIF-8 powder, methylcellulose, and bentonite are mixed with water to form a printable paste for additive manufacturing. Reprinted with permission [150]. Copyright 2019, American Chemical Society.

3.6.3. Advances in high-precision 3D printing with MOFs

Beyond ink regulation and structural functionalization, advancements in high-precision 3D printing technologies are propelling the development of novel MOF-based materials with complex structures and enhanced functionalities. One notable advancement is the use of two-photon polymerization for 3D printing of intricate structures within MOFs single crystals, demonstrating new capabilities for the precise manipulation of MOF materials [156]. This opens up new possibilities for fabricating advanced materials with tailored properties. Additionally, the integration of metal 3D printing with surface chemical engineering of MOFs has been shown to enhance liquid-phase catalytic hydrogen production, further enhancing the potential of MOF-based materials for energy conversion applications [157]. These advancements highlight that high-precision 3D printing technologies not only facilitate the creation of complex architectures but also impart novel functional properties to materials, paving the way for future applications in energy storage, conversion, and beyond.

3.7. Rheomechanical mechanism analysis of MOF-based materials in 3D printing

3.7.1. Interaction mechanisms between components

The synergistic effects between MOFs and matrices are primarily manifested in electrostatic interactions, hydrogen bonding networks, physical crosslinking, and additive modulation mechanisms. MOF particles (*e.g.*, MOF-525, ZIF-8) form interconnected networks with matrices (*e.g.*, cellulose nanocrystals (CNC), Pluronic F127) through electrostatic interactions, thereby enhancing the mechan-

ical properties of energy storage materials. For instance, the electrostatic interactions between MOF-525 and CNC in deep eutectic solvents (DES) significantly improve the storage modulus (G') and yield stress of the composite [92]. Additionally, hydrogen bonding interactions (*e.g.*, between ZIF-8 and TEMPO-oxidized cellulose nanofibers (TOCNF)) enhance the viscoelasticity of the ink, facilitating the formation of self-supporting gel structures [121]. MOFs acting as nanofillers (*e.g.*, HKUST-1 gels) can also integrate with polymer chains (*e.g.*, F127, PDMS) *via* van der Waals forces to construct rigid networks, effectively suppressing shear-induced deformations.In terms of additive modulation, crosslinkers (*e.g.*, *N*,*N*′-methylenebisacrylamide (MBA)) increase the Young's modulus by enhancing covalent crosslinking density. However, excessive crosslinking reduces toughness, as exemplified by the optimal toughness achieved at 0.5 mol% MBA [92]. Conversely, surfactants (*e.g.*, Pluronic F127) adsorb onto the hydrophobic surfaces of MOFs and form micellar networks through hydrophilic chains, stabilizing suspensions and amplifying shear-thinning effects. This mechanism plays a critical role in applications such as lithium-oxygen (Li-O_2) battery frameworks [102].

3.7.2. Correlation between rheological properties of MOF-based inks and 3D printing performance

Shear-thinning behavior is pivotal in the 3D printing of MOF-based inks. Its underlying mechanism involves the rupture of physical connections between MOF particles under high shear rates ($>100\,s^{-1}$), leading to a drastic viscosity reduction (*e.g.*, a three-order-of-magnitude drop in viscosity for MOF-Fe/SiC inks) to enable smooth extrusion. Upon shear cessation, the network rapidly self-heals, restoring viscosity (*e.g.*, G' recovery time < 1 s for HKUST-1 gels), ensuring shape fidelity [104,108]. High storage modulus ($G' > 10^4$ Pa) and yield stress ($\tau_y > 200$ Pa) are critical to suppressing filament collapse post-extrusion, guaranteeing stable interlayer stacking (*e.g.*, MOF-Fe/SiC inks with $G' = 10^5$ Pa and $\tau_y = 2.5 \times 10^3$ Pa). For elastically dominated inks ($G' > G''$, *e.g.*, Co-MOF-F127 gels with $G'/G'' \approx 10$), their anti-creep capability supports unsuspended architectures, making them suitable for applications such as Li-O_2 batteries [102]. Additionally, optimizing τ_y balances filament fusion and interlayer adhesion, as demonstrated by boehmite-based inks with 52 wt% solid content exhibiting optimal performance. Frequency-independent G' plateaus (*e.g.*, Co-MOF-F127) further ensure structural stability during printing, preventing layer misalignment caused by oscillations.

4. Applications of MOF-MXene composite functional materials in 3D printing

In recent years, multifunctional composite materials based on MOFs and MXene have demonstrated significant potential in energy storage and flexible electronic devices. Benefiting from their customizable porous structures, high specific surface area, and excellent electrical conductivity, researchers have combined innovative synthesis strategies with advanced manufacturing techniques, such as 3D printing and microfluidic regulation, to achieve precise multiscale structural design and performance optimization of MOF-MXene composites.

To address the challenges associated with the easy loss and difficulty of recycling traditional powder adsorbents, Shahriyari Far *et al.* [116] proposed a synergistic strategy combining *in situ* solvothermal synthesis and DLP 3D printing to fabricate hierarchically porous MXene/UiO-66 composite adsorbents. The solvothermal method enabled the *in-situ* growth of UiO-66 crystals on the surface of $Ti_3C_2T_x$ MXene nanosheets, enhancing the material's hydrophilicity and adsorption capacity. Meanwhile, DLP printing endowed the material with complex topological structures, optimizing fluid dynamics and significantly improving its dye removal efficiency and cycling stability.

In the field of zinc-ion batteries, Lu *et al.* [158] developed a microfluidics-assisted 3D printing (M3DP) technique to achieve the dynamic assembly of MXene/Cu-THBQ heterostructures and the uniform coating of Zn-P anodes. The synergistic effects of ultrasound and magnetothermal activation in the microfluidic channel facilitated the formation of conductive MOF-MXene heterointerfaces, optimizing Zn^{2+} flux distribution and suppressing dendrite growth. Furthermore, the M3DP technique enabled the fabrication of porous aerogel electrodes, which significantly enhanced the cycling lifespan of the battery.

For flexible electronic applications, Rana *et al.* [159] designed a multilayer textile-based triboelectric nanogenerator (M-TENG), leveraging the synergistic effects of MOF-525, Co-NPC, and MXene to achieve efficient charge generation, capture, and transport. MOF-525, with its high dielectric constant, enhanced charge density, while the porous Co-NPC layer served as a charge trap, and MXene nanosheets accelerated charge transport *via* a micro-capacitor effect. Additionally, 3D-printed biomimetic micropillar arrays increased the device's contact area, while hydrophobic surface modifications improved its environmental adaptability.

Furthermore, Zhou *et al.* [118,119] proposed a coordination engineering strategy to modulate the structure of MOF-based materials. By partially substituting Co^{2+} in Co-MOF with Ni^{2+}, followed by phosphidation, NiCoP multi-metallic phosphides were generated, leading to enhanced electron mobility and reduced charge transfer resistance. Utilizing 3D printing, NiCo-MOF@V_2O_5 composites were co-printed with MXene ink to construct interdigitated micro-supercapacitors, significantly improving areal capacitance and energy density.

Overall, the research on MOF-MXene composites is advancing toward precise structural modulation, multifunctional integration, and the convergence of advanced manufacturing techniques, providing new avenues for the development of high-performance energy storage devices and environmental remediation technologies.

5. Advanced applications of MXene- and MOF-based materials in 3D printed energy storage devices

The integration of MXene and MOF-based materials into 3D-printed structures holds transformative potential for energy storage devices, offering solutions to key challenges in scalability, performance, and design flexibility. MXene, a family of two-dimensional transition metal carbides and nitrides, exhibit a unique combination of properties that make them particularly well-suited for energy storage applications such as batteries [147,160–163] and supercapacitors [164,165]. Additionally, their inherent mechanical robustness and tunable surface functional groups, such as hydroxyl, fluorine, and oxygen, make them highly versatile for diverse applications. The ability to form stable, printable inks further highlights their compatibility with advanced manufacturing processes like 3D printing, enabling the fabrication of complex and customizable energy storage architectures with enhanced performance.

Similarly, MOFs provide complementary advantages through their highly porous structures, extraordinary surface areas, and flexible chemical compositions. These attributes allow MOFs to act as efficient hosts for active species or facilitate ion transport within energy storage devices. Their tunable pore size and chemistry make them suitable for optimizing ion diffusion pathways, which is critical for improving energy density and cycling stability. Furthermore, MOF-based materials can be integrated into hybrid systems, enhancing the electrochemical properties of MXene and other conductive substrates by providing additional active sites and improving charge transfer dynamics [116,166–169].

The synergy between MXene and MOFs opens up exciting opportunities for designing hybrid materials that leverage the strengths of both components. For instance, MXene can enhance electrical conductivity in MOF-based systems, while MOFs can provide additional pathways for ion transport and storage, addressing the limitations of each material individually. When integrated into 3D-printed architectures, these materials enable precise control over device design and geometry, unlocking new possibilities for custom-tailored energy storage solutions. Moreover, the combination of MXene and MOFs aligns with the growing demand for scalable, sustainable, and high-performance materials in energy technology. The ability to engineer these materials into complex 3D structures through printing technologies such as inkjet, extrusion, or SLA makes them highly suitable for advanced applications, including wearable electronics, portable power sources, and grid-level energy storage systems.

In the following sections, we delve deeper into the advantages of MXene- and MOF-based materials, categorizing their applications across various electrochemical devices. Key findings from the literature will highlight their performance metrics, practical challenges, and future prospects, providing a comprehensive understanding of their role in shaping the future of energy storage.

5.1. MXene-based applications in 3D printing

5.1.1. MXene-based supercapacitors

MXene, a class of 2D transition metal carbides, nitrides, or carbonitrides, have become a promising material for supercapacitors due to their exceptional electrical conductivity, tunable surface chemistry, and mechanical strength. These properties enable fast charge/discharge rates, high power density, and long cycle life, which are crucial for supercapacitor performance. The high conductivity of MXene ensures rapid electron transport, while their large surface area provides numerous active sites for energy storage, enhancing capacitance of supercapacitors. Moreover, their surface chemistry can be tailored with functional groups such as –OH, –F, and –O, optimizing their interaction with electrolytes and improving ion adsorption. Additionally, the remarkable mechanical strength of MXene ensures the structural integrity of supercapacitors during prolonged cycling. In 3D-printed supercapacitors, MXene excel due to their ability to form stable inks with high conductivity, allowing for the fabrication of complex, customizable geometries that increase surface area and electrolyte penetration. This results in improved performance and the ability to create supercapacitors with tailored form factors for specific applications, such as wearable or flexible electronics. Furthermore, MXene are ideal for MSCs, which are small-scale, high-performance devices used in portable electronics applications. 3D printing enables precise control over the design of these MSCs, ensuring they meet the power and energy demands of compact devices. Together, MXene and 3D printing offer a versatile approach to creating advanced, high-performance supercapacitors for the next generation of energy storage applications.

MSCs have emerged as a vital application area for MXene-based materials in 3D printing, primarily due to their high power density, long cycle life, and exceptional energy storage capabilities [43,170,171]. For example, additive-free 2D $Ti_3C_2T_x$ MXene ink was utilized to fabricate MSCs, achieving ultra-high energy densities. This advancement demonstrated ability of MXene to deliver exceptional electrochemical performance without the need for additional conductive additives, simplifying the ink formulation process. A critical aspect highlighted in this work is the optimization of ink viscosity and printability, which are essential for producing high-resolution 3D structures with enhanced energy storage characteristics. Further advancing this field, the direct 3D printing of MSCs using additive-free MXene inks has demonstrated both scalability and adaptability. These inks enabled the construction of complex micro-architectures, while maintaining excellent electrochemical properties (Fig. 16a) [42]. A notable challenge addressed in this work was balancing ink rheology to meet the dual demands of printability and electrochemical performance, a common challenge in MXene-based 3D printing research.

Another significant breakthrough involved the fabrication of high-voltage aqueous MSCs *via* 3D printing, achieving ultrahigh areal energy density and demonstrating robust low-temperature performance (Fig. 16d) [172]. This research exemplified the versatility of MXene-based inks across diverse environmental conditions. The ability to fine-tune MXene surface chemistry through 3D printing techniques further enhances ionic conductivity and energy storage, positioning MXene as a promising material for next-generation MSCs.

Beyond MSCs, MXene-based materials have demonstrated immense potential in hybrid capacitors [68,69]. The 3D printing of porous nitrogen-doped $Ti_3C_2T_x$ MXene scaffolds has enabled the development of high-performance sodium-ion hybrid capacitors. Nitrogen doping enhances electronic conductivity and electrochemical activity, significantly improving energy storage performance. This advancement underscores the importance of 3D printing in controlling the porosity and surface area of MXene-based materials, which are critical factors in optimizing the functionality and efficiency of hybrid capacitors.

Similarly, the development of 3D-printed Zn-ion hybrid capacitors using divalent cation-gelated additive-free $Ti_3C_2T_x$ MXene ink has highlighted the promising potential of MXene in multi-valent ion storage [69]. These devices offer superior energy densities and extended cycle lives, paving the way for advanced energy storage devices. Such progress highlights the adaptability of MXene-based materials for a wide range of next-generation energy storage technologies.

The inherent flexibility and mechanical robustness of MXene-based materials have been effectively utilized in the development of innovative flexible energy storage devices [64]. Advances in 3D printing have enabled the creation of stretchable MSCs with outstanding areal performance, demonstrating the adaptability of MXene inks for wearable and portable electronics. This approach emphasizes the importance of optimizing the mechanical properties of MXene-based materials to achieve a balance between high electrochemical performance and mechanical stability.

Additionally, functionalization of 3D-printed MXene electrodes has emerged as a key strategy for enhancing the performance of flexible electrochemical capacitors [62]. By tailoring the surface properties of MXene, researchers have improved the capacitive performance, durability, and flexibility of energy storage devices. These developments highlight the potential of MXene-based materials in producing high-performance, flexible energy storage solutions.

In brief, MXene-based materials represent a versatile and powerful class of materials for 3D-printed electrochemical energy storage in supercapacitors. Their unique combination of electrical conductivity, tunable surface chemistry, and mechanical properties makes them ideal candidates for a wide range of applications, from MSCs to hybrid capacitors and flexible energy storage devices. The existing literature highlights the importance of optimizing ink formulation, printability, and material functionalization to fully exploit the potential of MXene in 3D printing. As the field continues to evolve, future research should focus on addressing challenges such as long-term stability, scalability, and further enhancement of electrochemical performance, paving the way for widespread adoption of MXene-based 3D-printed energy storage devices in diverse applications.

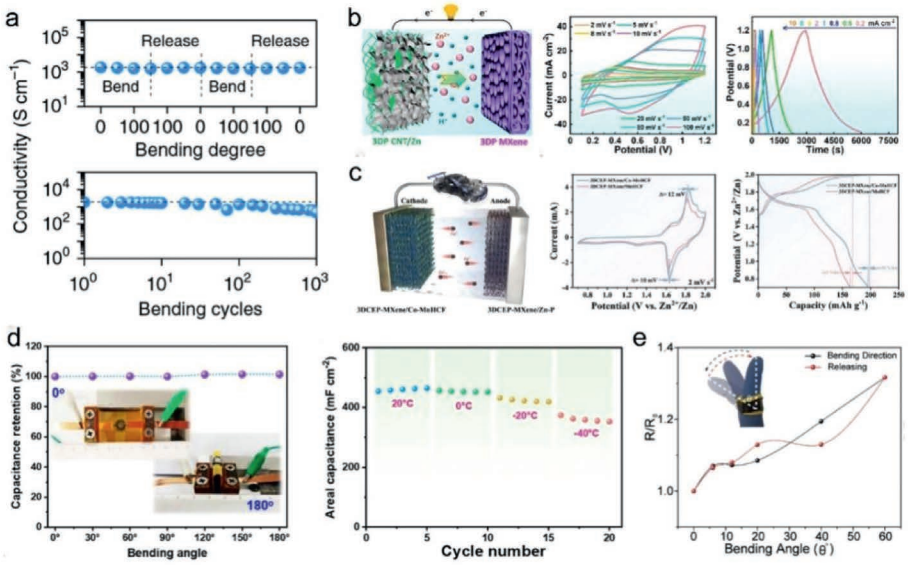


Fig. 16. Advancements in 3D-printed MXene-based MSCs and sensing devices: Performance, flexibility, and scalability. (a) Electronic conductivity of extrusion-printed $Ti_3C_2T_x$ MXene lines plotted as a function of bending degree (top) and bending cycles (bottom), demonstrating the material's flexibility and durability. Reprinted with permission [42]. Copyright 2019, Nature. (b) Electrochemical performance of dual-ion storage 3D-printed $Ti_3C_2T_x$ MXene cathodes, highlighting enhanced performance through pseudocapacitive and double-layer capacitive behaviors. Reprinted with permission [69]. Copyright 2021, American Chemical Society. (c) Investigation of electrochemical properties and reaction kinetics of 3D-printed full cells, showcasing their potential for high-performance energy storage. Reprinted with permission [44]. Copyright 2022, Wiley-VCH. (d) Integration of 3D-printed MSCs and their robust low-temperature electrochemical performance, demonstrating scalability and environmental adaptability. Reprinted with permission [172]. Copyright 2024, Wiley-VCH. (e) The printed $Ti_3C_2T_x$ MXene device responding to finger motions at different bending angles, highlighting the material's potential in flexible and wearable sensor applications. Reprinted with permission [48]. Copyright 2021, Wiley-VCH.

5.1.2. Advanced batteries with MXene components

MXene have emerged as a promising solution for battery technologies due to their unique combination of electrochemical properties and structural versatility. Their layered structure facilitates precise control over ion intercalation pathways, enabling efficient energy storage and rapid charge/discharge cycles. This capability sets MXene apart from traditional electrode materials, offering superior ion accessibility and transport dynamics, making them integral to next-generation battery systems. A standout feature of MXene is their exceptional structural stability, which ensures prolonged cycling durability even under high-capacity energy demands. This resilience, combined with their excellent electronic conductivity, minimizes internal resistance and delivers consistent battery performance. Moreover, their surface chemistry is highly tunable, allowing the incorporation of functional groups such as –OH, –O, and –F. This customization enhances ion adsorption and desorption processes, boosting overall energy efficiency and capacity.

In the realm of 3D-printed batteries, MXene provide transformative potential. Their compatibility with advanced printing technologies enables the fabrication of intricately structured electrodes with enhanced surface areas and optimized porosity. These features facilitate effective electrolyte infiltration and maximize the utilization of active materials, critical for achieving higher energy densities and extended lifespans. For example, the fabrication of additive-free $Ti_3C_2T_x$ MXene microlattices has demonstrated the transformative potential of MXene-based materials in advancing 3D-printed battery devices [167]. The use of a template-assisted 3D printing method allows for the precise customization of microstructures, which is crucial for optimizing the electrochemical performance of battery electrodes. These MXene microlattices exhibit high areal capacitance, which is essential for improving energy density in compact and efficient battery designs.

One of the key innovations in this approach is the ability to tailor microstructures which significantly enhances the electrochemical surface area. This enhancement boosts both charge storage capacity and overall energy efficiency, contributing to the advancement of 3D-printed energy storage devices. Additionally, by eliminating additives during the fabrication process, the MXene microlattices maintain their inherent conductivity and electrochemical activity, ensuring maximum performance in energy storage applications [47]. Furthermore, the template-assisted 3D printing technique is scalable and adaptable, supporting the mass production of battery components with consistent performance metrics, making it a promising solution for industrial applications. This combination of microstructural tailoring, additive-free design, and scalability highlights the potential of MXene in revolutionizing 3D-printed batteries.

The integration of these advancements is further exemplified in the development of a 3D printed $Ti_3C_2T_x$ MXene cathode (Fig. 16b), which employs a dual ion storage mechanism. This mechanism synergistically combines the pseudocapacitive behavior of H^+ ions and the double-layer capacitive behavior of Zn^{2+} ions which significantly optimize the electrochemical performance [69]. The resulting zinc ion hybrid capacitor exhibits enhanced carrier transport, easy electrolyte penetration, and sufficient porosity, leading to high capacitance and extended lifespan. In another study, a novel 3D cold-trap environment printing technique (Fig. 16c) was employed to further enhance the structural stability and longevity of aqueous Zn-ion batteries [44]. This innovative method addresses critical challenges such as electrode degradation during cycling, and provides notable advantages. For example, by integrating the cold-trap printing technique with MXene, electrode stability is significantly enhanced, a crucial factor for extending the lifespan of Zn-ion batteries. Furthermore, MXene effectively mitigate electrode degradation during charge-discharge cycles, ensuring reliable and long-term performance. From an environmental perspective, the combination of aqueous Zn-ion batteries with MXene supports sustainability goals, as these systems utilize non-toxic materials and water-based electrolytes.

These innovations collectively highlight the transformative impact of MXene-based materials in the field of 3D-printed battery

devices. By leveraging the unique properties of MXene, researchers can achieve significant improvements in battery performance, including higher energy densities, enhanced longevity, and structural customization. The continued exploration of MXene-based materials in 3D printing technologies promises to further advance the development of next-generation battery devices with superior electrochemical performance.

5.1.3. Wearable sensing devices enabled by MXene

MXene-based materials have emerged as highly promising candidates for 3D-printed wearable sensing devices due to their exceptional electrical conductivity, mechanical strength, and chemical stability. These properties make MXene ideal for sensors that require real-time, high-performance data collection in wearable applications. Unlike traditional materials, MXene enable the formation of intricate microstructural patterns during 3D printing. These patterns significantly enhance the sensitivity, electrical properties, and response speed of the sensors, making them indispensable for next-generation wearable devices.

A distinguishing feature of MXene is their tunable surface chemistry, which allows precise interaction with specific target molecules. This customization ensures high selectivity and sensitivity, making MXene versatile for various types of wearable sensor applications. For example, combining advanced manufacturing techniques like freeze-drying and 3D printing has led to the development of hierarchical MXene pressure sensors with porous structures. These innovations improve sensitivity and durability, particularly under high-pressure conditions, thereby addressing critical requirements for real-world applications.

Recent studies have demonstrated the effective 3D micropatterning of $Ti_3C_2T_x$ MXene using advanced additive manufacturing techniques, achieving intricate microstructures (Fig. 16e) [48]. Precise control of printing parameters in these studies resulted in finely tuned microstructures with superior high electrical conductivity and mechanical strength. These advancements highlight the potential of MXene-based materials to redefine sensor performance by significantly enhancing sensitivity, electrical properties, and response speed. Moreover, the ability to fabricate high-resolution and complex geometries expands the scope of MXene in advanced sensing technologies, paving the way for transformative innovations in wearable sensors.

The rheological properties of MXene dispersions are critical for achieving precise 3D printing of wearable sensors. Key factors, such as ink flowability, viscosity, and shear-thinning behavior, directly influence the resolution, uniformity, and structural stability of the printed sensors. Optimization of these properties ensures smooth extrusion and consistent performance during the printing process [49]. For example, enhanced ink flowability enables accurate deposition, while controlled viscosity supports proper layer stacking, critical for fabricating intricate sensor designs. Such improvements reduce defects like clogging or uneven deposition, enhancing the structural integrity and functionality of the sensors. Moreover, maintaining high conductivity and mechanical stability further underscores the practical viability of MXene-based wearable sensors.

Advancements in 3D printing techniques have also enabled the fabrication of MXene scaffolds with complex geometries, such as gyroid structures, which exhibit exceptional mechanical sensitivity [51]. These structures achieve ultra-high sensitivity for microscale strain detection, which is essential requirement for wearable sensor applications. Such findings provide valuable insights into the design and manufacturing of next-generation wearable sensors, paving the way for significant advancements in this rapidly evolving field.

Hierarchical MXene-based pressure sensors represent another breakthrough, combining the excellent electrical conductivity and mechanical strength of MXene with freeze-drying techniques to create a porous hierarchical structures [45]. This novel approach significantly improves sensitivity and durability of pressure sensors, particularly under high-pressure conditions. The integration of 3D printing and freeze-drying offers an innovative solution for creating highly sensitive and durable wearable pressure sensors. These sensors hold immense potential for real-world applications such as health monitoring and tactile sensing, where precision and durability are paramount.

In conclusion, MXene-based materials, when coupled with advanced manufacturing techniques, provide a versatile platform for developing next-generation wearable sensors. By leveraging their unique properties and addressing challenges in 3D printing, MXene can revolutionize the field of wearable sensing devices, offering unparalleled performance and scalability for diverse applications.

5.1.4. MXene-based hybrid systems for multifunctional applications

MXene have emerged as highly versatile materials, with several studies demonstrating their integration into hybrid systems to enhance both mechanical and electrochemical properties [29]. For example, composites of MXene with cellulose nanofibers or graphene exhibit improved structural integrity and superior energy storage capabilities. These findings highlight MXene' adaptability, positioning them as key materials for addressing challenges in energy storage and conversion technologies.

Building on this versatility, MXene play a dual role in multifunctional devices, serving as both a structural reinforcement and an active electrochemical component. When coupled with advanced fabrication techniques like 3D printing, the potential of MXene-based materials is further amplified. 3D printing enables precise engineering of complex architectures, unlocking unprecedented opportunities for next-generation energy systems with tailored performance metrics.

5.2. MOF-based martials breakthroughs in 3D printing

MOF-based materials are revolutionizing the field of 3D-printed energy storage and conversion devices due to their high surface area, tunable porosity, and versatile chemical functionality. These unique features enable MOF-based materials to optimize ion transport, improve energy densities, and enhance the overall efficiency of devices such as batteries, supercapacitors, and catalytic systems. By leveraging advanced 3D printing technologies, MOF-based materials can be fabricated into intricate geometries with precisely controlled porosity, which not only maximizes material utilization but also ensures improved electrochemical efficiency.

Moreover, the integration of MOF-based materials into 3D-printed devices provides innovative solutions to long-standing challenges in traditional manufacturing techniques. Unlike conventional methods, 3D printing offers scalability, reproducibility, and the ability to create complex structural designs tailored to specific energy applications. In addition, the versatility of these materials extends beyond energy storage to catalytic energy conversion. MOFs' chemically tunable frameworks enable the incorporation of active sites for reactions such as hydrogen evolution and oxygen reduction. Combined with the precision of 3D printing, MOF-based catalytic systems can achieve lightweight, porous architectures with exceptional durability and performance [173]. These advancements highlight the enormous potential of MOF-based materials in addressing critical challenges in energy technologies, positioning them as indispensable materials in the development of next-generation energy solutions.

5.2.1. MOF-based battery technologies

MOFs have garnered significant attention in recent years due to their exceptional properties, including high surface area, tunable

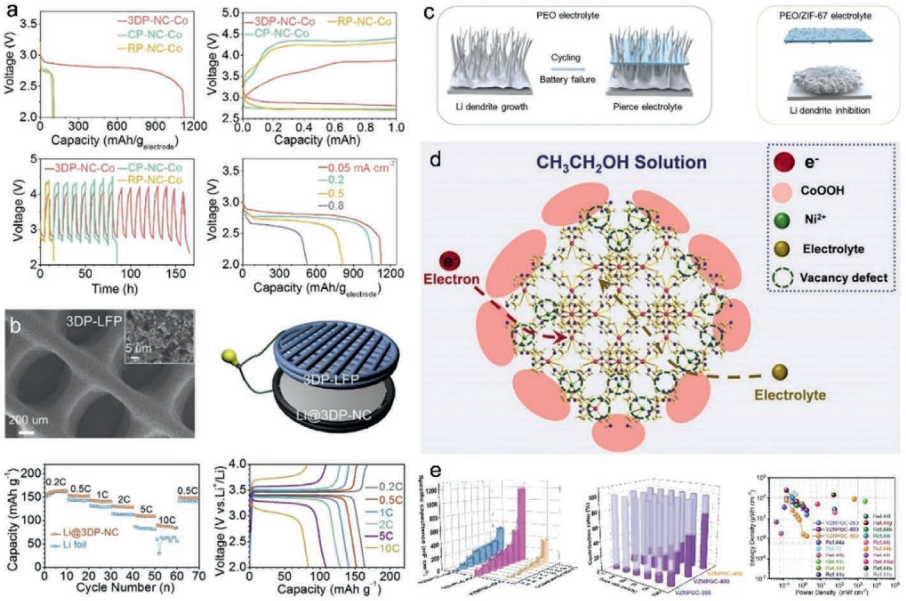


Fig. 17. Advancing energy storage: The role of MOF-based 3D printing. (a) Electrochemical performances of 3D-printed nitrogen-doped carbon-cobalt (3DP-NC–Co) materials. Reprinted with permission [102]. Copyright 2022, Wiley-VCH. (b) Rate performance of the full cell using the Li@3DP-NC anode and the 3DP-LiFePO4 cathode. Reprinted with permission [103]. Copyright 2019, Elsevier. (c) Comparison of lithium dendrite growth in PEO/L electrolyte *versus* inhibition in PEO/L-5Z electrolyte. Reprinted with permission [146]. Copyright 2023, Wiley-VCH. (d) Schematic illustration of the ion transport mechanism in MOF-based MSCs. Reprinted with permission [118]. Copyright 2023, Wiley-VCH. (e) Electrochemical comparison of VZNPGC//MXene MSCs. Reprinted with permission [119]. Copyright 2024, Wiley-VCH.

porosity, and chemical versatility. These attributes make them ideal candidates for fabricating advanced battery devices. In particular, MOFs offer unique advantages in tailoring material architecture and optimizing ion transport pathways, which are critical for improving the performance of energy storage and conversion systems [169,174–176]. This section explores the role of MOF-based materials in 3D-printed battery technologies, focusing on their ability to enhance energy density, charge-discharge efficiency, and overall device performance.

Hierarchical porous MOF-derived frameworks for high-energy density Li–O_2 batteries: Recent research has explored the development of 3D-printed MOF-derived hierarchically porous frameworks designed for high-energy density Li–O_2 batteries (Figs. 17a and b) [102,103]. The unique structural characteristics of MOFs, such as high surface area and tunable porosity, are leveraged to fabricate battery electrodes that significantly enhance energy density. The hierarchical porosity of the frameworks facilitates efficient oxygen diffusion and electrolyte accessibility, leading to optimized overall battery performance. This advancement highlights the transformative potential of MOF-based 3D printing technologies in achieving superior performance in energy storage applications.

In a related development, researchers have successfully designed 3D-printed electrodes for lithium metal batteries that exhibit high areal capacity and exceptional rate capability [172]. By integrating MOF materials into the electrode structures, critical challenges such as dendrite growth and electrode degradation are addressed. This investigation highlights how MOF-based 3D printing can significantly improve the performance metrics of lithium metal batteries, paving the way for more efficient and durable energy storage solutions.

Further advances have been achieved in lithium–sulfur batteries through the development of a 3D-printed aluminum MOF/S cathode [112]. The optimized MOF framework enhances polysulfide adsorption and redox conversion, effectively mitigating polysulfide dissolution, which is a common challenge in these systems. This advancement leads to the development of a more stable and high-performance cathode, demonstrating the potential of MOF-based structures in overcoming technical barriers to lithium–sulfur battery advancement.

Beyond cathode and electrode design, 3D printing has also been applied to the fabrication of porous MOF-based hybrid solid-state electrolytes. A universal room-temperature printing method was introduced to inhibit dendrite formation in SSBs (Fig. 17c) [146]. The porous architecture of MOFs not only ensures robust ionic conductivity but also addresses safety concerns associated with dendrite growth, making SSBs more reliable and efficient. This approach demonstrates the potential of MOF-based 3D printing in creating next-generation solid-state electrolytes with enhanced performance.

Another innovative application involves the design of 3D printed grid reservoir-integrated anodes for ZIBs. These anodes, enriched with MOF-based materials, improve both battery longevity and safety by mitigating dendrite formation [147]. The grid reservoir structure ensures uniform zinc deposition, further enhancing the stability of the battery system. This study exemplifies how MOF-based 3D printing can address safety challenges while maintaining high performance in ZIBs.

In summary, the integration of MOF-based materials into 3D printing technologies for battery devices has unlocked significant advancements across multiple domains of energy storage. From enhancing energy density in Li–O_2 batteries to improving electrode performance, managing polysulfide dissolution in lithium–sulfur systems, and mitigating dendrite formation in solid-state and ZIBs, MOFs offer unparalleled versatility and effectiveness. These breakthroughs lay a strong foundation for future exploration of MOF-based 3D printing technologies.

5.2.2. Supercapacitors with MOF-based 3D printing

Supercapacitors demand materials with high surface area, excellent conductivity, and long-term stability to achieve superior energy storage performance. MOF-based materials, with their customizable porosity and tunable chemical properties, emerge as promising candidates for integration into 3D-printed supercapacitor architectures. When employed in these structures, MOFs sig-

nificantly enhance energy density and charge-discharge rates, addressing key limitations of conventional materials.

A notable example is the synergistic enhancement of supercapacitor performance by incorporating of Ni^{2+} and cobalt-based organic frameworks into 3D-printed MSCs (Fig. 17d). The unique combination of these frameworks with advanced printing techniques achieved remarkable improvements in specific capacitance and extended the cycle life of the device [118]. Furthermore, utilization of Ni^{2+} ions within hollow nano-MOFs, followed by their hybridization with polymetallic phosphides, further boosts electrochemical performance. This approach optimizes electron transfer and ion diffusion pathways, significantly increasing energy and power densities (Fig. 17e) [119]. The precision enabled by 3D printing is a critical factor in these enhancements, as it allows precise control over the material's morphology, ensuring efficient transport of charge carriers. These advancements showcase how MOF integration can effectively harness the potential of additive manufacturing for next-generation energy storage.

MOF-based materials have also been successfully combined with graphene aerogels in 3D-printed electrodes for hybrid supercapacitor-battery devices [120]. This composite structure provides an optimal balance between high energy and power density, illustrating the high conductivity of graphene and the tunable porosity of MOFs. Such integration not only improves electrochemical performance but also broadens the range of applications for MOF-based materials, particularly in devices requiring rapid charge-discharge capabilities and extended cycle life.

5.2.3. Catalysis innovations with MOF-integrated 3D printing

MOFs have shown considerable promise in advancing 3D printing technologies for catalytic applications. The integration of MOFs into 3D-printed materials have achieved significant enhancements in catalytic performance across diverse processes. The synergy between MOFs intrinsic properties and the design freedom offered by 3D printing has led to remarkable progress in catalysis, paving the way for innovations in sustainable energy and chemical manufacturing [177–179]. The following discussion explores key developments in three primary domains where MOF-based 3D printing has demonstrated exceptional promise: Hydrogen storage, photocatalysis, and catalytic reactions. These developments highlight how the integration of MOFs into 3D-printed systems is reshaping catalytic science, enabling breakthroughs that were previously unattainable with traditional materials and fabrication methods. Through these advancements, MOF-based 3D printing is not only addressing contemporary challenges in catalysis but is also redefining the boundaries of material science and engineering.

MOF-based materials are increasingly utilized in 3D printing for developing advanced hydrogen storage solutions. MOF composites embedded in 3D-printed matrices, such as ABS-MOF composites, control the inherent high surface area and tunable porosity of MOFs [100]. These properties enable efficient hydrogen adsorption and desorption, leading to substantial improvements in storage capacity and system performance. This innovative approach bridges the gap between material functionality and practical implementation, marking a significant advancement in the development of scalable hydrogen storage solutions.

Recent advancements in MOF-based photocatalysis showcased their potential to enhance hydrogen generation. 3D-printed MOF-derived composites allow precise control over the printing process and material structure, optimizing photocatalytic activity [101]. The inherent high surface area and well-defined architectures of MOFs contributes contribute significantly to improved photocatalytic efficiency. These features position MOF-based materials as pivotal components in the design of sustainable hydrogen production systems. By utilizing 3D printing, researchers can tailor MOF structures for enhanced light absorption and catalytic performance, offering a pathway to more efficient and environmentally friendly energy solutions.

3D-Printed MOF-based materials have also demonstrated significant potential in advancing catalytic reactions and reactor design, with diverse applications showcasing their versatility. For example, the fabrication of 3D-printed Fe/γ-Al_2O_3 monoliths incorporating MOF-derived structures has improved catalytic activity for the hydroxylation of phenol [104]. This is achieved through improved dispersion and accessibility of active sites, highlighting the effectiveness of MOF-based 3D printing in producing high-performance and durable catalytic materials. Additionally, the fabrication of 3D-printed porous magnetic carbon materials derived from MOFs, which combine high catalytic activity with magnetic properties, has highlighted the versatility of MOF-based materials in multifunctional catalyst design [105]. The ability to facilitate catalyst recovery and reuse further enhances the practicality of these materials across various catalytic processes. Moreover, the integration of MOFs directly onto polymeric supports through one-pot growth techniques has been shown to significantly boost catalytic performance in CO_2 conversion processes, contributing to both efficiency and stability in these processes [140]. This approach illustrates how MOF-based 3D printing can be leveraged to create advanced catalysts for CO_2 conversion, aligning with sustainability goals. In another innovative application, metal 3D-printed flow reactors, modified with MOF-based surface chemistry, have been engineered to optimize liquid-phase catalytic hydrogen production [157]. The enhanced catalytic performance and selectivity achieved in these reactors underscore the transformative role of MOF-based 3D printing in refining reactor design for industrial hydrogen production.

The advancements in MOF-based 3D printing for catalytic applications illustrate the significant potential of these materials in enhancing catalytic processes and reactor designs. From hydrogen storage and photocatalysis to catalytic reactions and reactor engineering, MOFs offer distinct advantages such as high surface area, tunable porosity, and multifunctionality. These developments not only improve catalytic efficiency but also open new avenues for future research and practical applications in various catalytic technologies.

6. Challenges and future perspectives

Despite these advancements, several challenges must be addressed to fully realize the potential of MXene- and MOF-based 3D printing. Ink formulation, for instance, remains a key hurdle, but recent progress in additive-free and ionic liquid-based systems offers promising solutions. Similarly, balancing porosity and structural integrity is critical, necessitating innovative approaches in material design and printing techniques. Addressing these challenges will require interdisciplinary collaboration and a focus on sustainable manufacturing processes.

6.1. Overcoming current challenges

The success of 3D printing MXene and MOF-based materials hinges on developing inks with precisely optimized rheological properties. Achieving a balance between viscosity, printability, and mechanical stability remains a persistent challenge. Additives are often introduced to improve rheological behavior, but these can compromise the intrinsic properties of MXene and MOFs, such as electrical conductivity and porosity, both of which are crucial for electrochemical applications. Therefore, the development of additive-free or minimally modified ink formulations that retain these functional properties without compromising printability is ongoing area of research. Furthermore, ensuring uniform dispersion of MXene and MOFs within the ink matrix is essential to

prevent aggregation, which can otherwise lead to performance inconsistencies and structural defects in printed materials.

Balancing porosity and mechanical strength poses another critical challenge. For energy storage and conversion devices, high porosity is desired to enhance ion transport and surface area. However, increasing porosity can weaken the mechanical integrity of the printed structures, making them susceptible to collapse or degradation under operational stresses. This trade-off emphasizes the need for innovative design strategies to create robust yet porous structures that can withstand repeated charge-discharge cycles and harsh environmental conditions without compromising performance.

While laboratory-scale demonstrations of MXene and MOF-based 3D-printed devices have shown promising results, scaling up these processes to industrial levels remains a significant challenge. Issues such as reproducibility, throughput, and cost-effectiveness of 3D printing techniques need to be addressed to make these technologies viable for large-scale energy storage and conversion applications. Moreover, the integration of these printed components into existing manufacturing workflows and device architectures poses additional hurdles. Addressing these issues requires an intensive effort to bridge the gap between laboratory-scale innovation and large-scale industrial implementation.

The long-term stability of MXene and MOF-based materials under operational conditions is another area of concern. MXene are particularly susceptible to oxidation, which significantly diminishes their performance over time. Similarly, MOFs may suffer from structural collapse or chemical degradation when exposed to challenging environmental conditions, such as high humidity or elevated temperatures. To improve durability, various strategies are being explored, including surface passivation, encapsulation, or the incorporation of stabilizing agents. Advancing these techniques will be critical for the practical deployment of these materials in energy storage devices.

The interfaces between the 3D-printed materials and other components of the energy storage device, such as current collectors, electrolytes, and separators, plays a critical role in overall device performance. Ensuring strong interfacial adhesion and minimizing contact resistance are crucial for enhancing efficiency. Additionally, the chemical compatibility of MXene and MOFs with various electrolytes needs careful consideration, as adverse interfacial reactions can lead to material degradation and a loss of performance. Therefore, engineering stable, low-resistance interfaces is essential for the development of reliable energy storage devices.

6.2. Future perspectives

Future research should focus on developing novel ink formulation strategies that leverage the unique properties of MXene and MOFs while overcoming current limitations. Future efforts should emphasize the use of green solvents, ionic liquids, or hybrid inks that combine the benefits of multiple materials. For instance, green solvents can minimize environmental impact while maintaining ink stability, whereas hybrid inks can combine the conductivity of MXene with the porosity and high surface area of MOFs for enhanced performance. Additionally, exploring self-assembly and directed assembly techniques during the printing process can facilitate the development of controlled and hierarchically structured materials, resulting in superior uniformity and functionality in printed devices.

The integration of MXene and MOFs into multifunctional 3D-printed architectures offers exciting opportunities for enhancing device performance and reducing system complexity. These architectures can be designed to perform multiple roles simultaneously, such as combining energy storage with catalytic activity, thermal management, or sensing capabilities. By leveraging the tunable properties of MXene and MOFs, researchers can create next-generation devices that enhance functionality while minimizing the need for additional components. Such advancements could revolutionize energy storage technologies, offering unprecedented versatility and efficiency.

The combination of MXene and MOFs with other functional materials, such as graphene, carbon nanotubes, or conductive polymers, could further enhance their performance in energy storage and conversion applications. By blending the best properties of each component, such as the high conductivity of MXene and the high surface area of MOFs, hybrid materials can achieve superior performance in energy storage and conversion applications. Additionally, the use of 3D printing to create gradient or layered structures with different material compositions could enable more efficient utilization of each material's properties and further optimizing device functionality.

As the field of 3D printing for energy storage and conversion matures, sustainability becomes a central focus. The development of eco-friendly materials, solvent-free printing techniques, and recycling strategies for end-of-life devices will be essential for the long-term viability of this technology. Research efforts should prioritize the use of biodegradable or renewable precursors for MXene and MOFs, and develop low-energy fabrication processes. These advancements could contribute to more environmentally friendly energy storage solutions, addressing both performance and ecological concerns.

Finally, translating laboratory-scale innovations into real-world applications will require collaboration between material scientists, engineers, and industry stakeholders. Addressing practical challenges such as device integration, reliability testing, and regulatory approvals is essential for enabling the widespread adoption of MXene- and MOF-based technologies. The establishment of standardized testing protocols and benchmarks for evaluating the performance of 3D-printed energy storage devices will be crucial for gaining industry acceptance and facilitating commercialization. The integration of artificial intelligence (AI) with MXene- and MOF-based composite materials heralds a paradigm shift in collaborative hierarchical material-structure design. Advanced AI systems, exemplified by DeepSeek's multiscale modeling platform, enable precise analysis of material properties and optimization of synthesis strategies through predictive frameworks spanning atomic-scale interactions to macroscopic architectures. Machine learning models decipher MXene's surface termination dynamics (-O/-F ratio modulation) and MOF's coordination chemistry, achieving atomic-level hybridization for tailored electron/ion dual-transport networks. Simultaneously, generative AI (*e.g.*, diffusion models) optimizes 3D-printed mesoscale porosity (10 nm–10 μm), ensuring spatial alignment between MXene's conductive pathways and MOF's molecular-sieving domains, thereby resolving the historical conductivity-porosity trade-off. Reinforcement learning (RL) agents dynamically adjust MXene delamination parameters (*e.g.*, HF concentration, intercalants) and MOF crystallization conditions (*e.g.*, solvent polarity, nucleation kinetics) to engineer interfaces with $<5\%$ lattice mismatch. At the application level, AI-driven strain-field simulations synergize MXene's mechanical durability with MOF's dynamic bond reconfiguration, enabling foldable supercapacitors that retain 90% capacitance after 10^4 bending cycles. This AI-enhanced design philosophy transcends conventional trial-and-error methodologies by establishing causal relationships among molecular motifs, processing parameters, and macroscopic performance, thereby advancing the "materials-by-computation" paradigm. Ultimately, AI-powered digital twin ecosystems will allow MXene-MOF composites to undergo computational refinement prior to physical synthesis, accelerating their deployment in next-generation energy storage and conversion technologies.

Table 1
Comparison of material properties.

3D printing process	Electrode materials	Electrolyte	Specific capacitance/areal capacities	Current density/ scan rate	Energy density	Power density	Retention capacity (cycle number)	Ref.
DIW	MXene	PVA/H_2SO_4 gel electrolyte	79 mF/cm^2	50 mV/s	2 μWh/cm^2	0.6 mW/cm^2	94 % (10,000)	[45]
DIW	MXene	2 mol/L $ZnSO_4$	259.7 F/g	0.1 A/g	0.10 mWh/cm^2	5.90 mW/cm^2	86.5 % (6000)	[69]
DIW	3DP-NC//3DP-$LiFePO_4$	1 mol/L LiTFSI/DOL/DME (1 % $LiNO_3$)	30 mAh/cm^2	10 mA/cm^2	–	–	97.9 % (2000 h)	[103]
DIW	VZNGC-60//MXene	KOH-poly(vinyl alcohol) (PVA) gel electrolyte	585 mF/cm^2	0.48 mA/cm^2	159.23 μWh/cm^2	0.34 mW/cm^2	–	[118]
DIW	VZNPGC-400//MXene	KOH-poly(vinyl alcohol) (PVA) gel electrolyte	1184 mF/cm^2	0.24 mA/cm^2	236.75 μWh/cm^2	0.14 mW/cm^2	–	[119]
DIW	LFP//PEO/L-5Z//Li	MOF@LiTFSI solid electrolyte	159.5 mAh/g	–	–	–	95 % (100)	[146]
DIW	3DP-MPC-SiOC@Zn//3DP-VO@Ti	3 mol/L $ZnSO_4$	–	0.1 A/g	41 Wh/kg	1.2 W/kg	95.5 % (10,000)	[147]
DIW	MXene//$LiFePO_4$	–	149.4 mAh/g	1 mA/cm^2	–	–	99.4 % (300)	[158]
DIW	MXene-PVOH	1 mol/L H_2SO_4	20.05 mF/cm^3	5 mV/s	14.95 mJ/cm^3	4.95 mW/cm^3	80 % (100)	[159]
DIW	Pd/AT-Ni/MOFDC	2 mol/L ethanol and 2 mol/L potassium hydroxide	1264.4 cm^2/mg	–	–	26.49 mW/cm^2	68 % (24 h)	[161]
Screen printing technique	RuO_2·xH_2O@MXen	PVA–KOH	864.2 F/cm^3	1 mV/s	13.5 mWh/cm^3	48.5 W/cm^3	90 % (10,000)	[162]
DIW	MXene	PVA/H_2SO_4 gel electrolyte	2.337 F/cm^2	10 mA/cm^2	207.81 μWh/cm^2	3.74 mW/cm^2	93.1 % (10,000)	[163]
FDM	MXene (Y-$Ti_3C_2T_x$)	PVA@H_2SO_4	28.3 mF/cm^2	–	0.63 μWh/cm^2	0.33 mW/cm^2	94.1 % (10,000)	[169]
DIW	3DCEP-MXene/Zn-P//3DCEP-MXene/Co-MnHCF	PAAm-Zn(OTf)$_2$	218.4 mAh/g	0.2 A/g	283.92 Wh/kg	141.96 W/kg	95.7 % (1600)	[173]
DIW	GNPs/GO	PVA/H_2SO_4 gel electrolyte	195.1 F/m^2	0.4 A/m^2	24.91 mWh/m^2	1199.34 mW/m^2	80.65 % (5000)	[180]
Screen printing	BCN/rGO	PVA/H_2SO_4 gel electrolyte	72.2 mF/cm^2	0.1 mA/cm^2	11 mWh/cm^2	1175 mW/cm^2	95 % (10,000)	[181]
DIW	MnO_x/CNT (5:3)	1 mol/L Na_2SO_4	183.94 mF/cm^2	0.5 mA/cm^2	–	–	76.40 % (2000)	[182]
DIW	MXene/GO/Lignosulfonate	3 mol/L H_2SO_4	72.1 mg/cm^2	–	505.3 μWh/cm^2	2.6 mW/cm^2	94 % (2000)	[183]
DIW	RGO	PVA/H_3PO_4 gel electrolyte	101 mF/cm^2	0.5 mA/cm^2	–	–	94.5 % (10,000)	[184]
DIW	CNT@MnO_2//Zn	1 mol/L $ZnSO_4$ + 0.1 mol/L $MnSO_4$	63 μAh/cm^2	0.4 mA/cm^2	–	–	–	[185]
DIW	PSS/CNT	PVA-H_2SO_4 gel electrolyte	990 mF/cm^2	1 mA/cm^2	0.065 mWh/cm^2	0.4 mW/cm^2	74.7 % (14,000)	[186]
DIW	Hollow graphene fibers, GFs	PVA/H_3PO_4/H_2O gel electrolyte	170.6 F/g	0.05 A/g	–	–	–	[187]
DIW	rGO/SiCN(O)	3 mol/L KOH	39 F/g	0.60 A/g	–	–	–	[188]
Plasma jet 3D printing technology	EG/CNT/AgNW	PVA-H_3PO_4	21.6 mF/cm^2	0.01 V/s	0.5–2 μWh/cm^2	2.5 mW/cm^2	93.1 % (2000)	[189]
DIW	rGO/KCu_7S_4	6 mol/L PVA/KOH	815.83 F/g	0.5 A/g	286 μWh/cm^2	2.16 mW/cm^2	92.16 % (2000)	[190]
DIW	V_2CT_x/rGO-CNT	1 mol/L $NaPF_6$ solution in diglyme	50 mAh/cm^2	5 mA/cm^2	–	–	99.54 % (3000)	[191]

By addressing these challenges and exploring innovative directions, the field of MXene and MOF-based 3D printing for energy storage and conversion holds immense promise. The continued evolution of this technology could lead to breakthroughs, contributing to a more sustainable and energy-efficient future.

7. Conclusion

In this review, we have explored the growing field of MXene- and MOF-based materials in 3D printing, particularly focusing on their roles in electrochemical energy storage and conversion devices. The synthesis, formulation, and integration of these advanced materials into 3D-printed architectures present unique opportunities and challenges for the future of energy technologies.

Compared to conventional 3D-printed carbon-based materials (*e.g.*, graphene, carbon nanotubes), the MXene-MOF hybrid system exhibits distinct electrochemical advantages rooted in its complementary design (Table 1) [45,69,103,118,119,146,147,158,159,161–163,169,173,180–191]. While graphene excels in electrical conductivity and carbon nanotubes demonstrate exceptional mechanical strength, neither achieves multifunctional integration at the electrode-electrolyte interface. MXene-MOF composites uniquely address this gap: The metallic conductivity of MXene nanosheets forms continuous electron transport channel, while the MOF framework enables molecular-scale ion regulation through programmable nanopores. This synergy enhances both charge transfer kinetics and ion-accessible surface area, a pivotal advancement unachievable with traditional carbonaceous materials. Furthermore, the inherent chemical versatility of MXene-MOF interfaces facilitates dynamic adaptation to diverse electrochemical environments, overcoming the structural rigidity of graphene/carbon nanotube systems. Such integrated functionality positions MXene-MOF architectures as a transformative solution for next-generation energy devices requiring coupled high energy-power density and operational stability.

MXene, with their exceptional electrical conductivity, mechanical flexibility, and tunable surface chemistry, have demonstrated significant potential in various electrochemical applications, from batteries to supercapacitors. MOFs, on the other hand, offer unparalleled porosity and structural diversity, making them ideal candidates for enhancing ion transport and storage capacities. However, the combination of these materials with 3D printing technologies brings forth a new level of complexity, where ink formulation, structural integrity, and device integration must be carefully optimized. The advancements in 3D printing technologies, such as FDM, SLA, and inkjet printing, have enabled the fabrication of intricate and highly functional devices. Yet, the translation of these techniques from laboratory-scale to industrial-scale applications remains a significant hurdle. The challenges associated with ink rheology, structural stability, scalability, and long-term performance require further research and innovation.

Looking forward, the continued development of hybrid and composite materials, advanced ink formulation techniques, and sustainable manufacturing processes will be essential for unlocking the full potential of MXene- and MOF-based 3D-printed devices. Additionally, the exploration of multifunctional architectures and real-world integration will pave the way for next-generation energy storage solutions that are both efficient and environmentally friendly.

In conclusion, while significant progress has been made in the field of MXene- and MOF-based 3D printing for electrochemical energy storage and conversion, there remains a vast landscape of opportunities for future research. The synergy between material science, 3D printing technology, and electrochemical engineering will continue to drive innovations that address the energy challenges of our time. As we move forward, interdisciplinary collaboration and a focus on scalability, sustainability, and performance optimization will be key to realizing the full impact of these technologies on the energy landscape.

CRediT authorship contribution statement

Huijie Zhou: Writing – review & editing, Writing – original draft, Visualization, Investigation, Data curation. **Mutawara Mahmood Baig:** Writing – review & editing, Writing – original draft. **Shunyu Gu:** Writing – review & editing, Writing – original draft. **Wenjiang Zou:** Writing – review & editing, Visualization. **Jing Zhang:** Writing – review & editing, Writing – original draft. **Fei Dou:** Writing – review & editing, Writing – original draft. **Jiang Xu:** Writing – review & editing, Writing – original draft. **Lvzhou Li:** Writing – review & editing, Writing – original draft. **Yizhou Zhang:** Writing – review & editing, Writing – original draft, Visualization. **Huan Pang:** Writing – review & editing, Writing – original draft, Investigation, Funding acquisition. **Jianning Ding:** Writing – review & editing, Writing – original draft, Investigation.

Declaration of competing interest

The authors declare that they have no known competing financial interests or personal relationships that could have appeared to influence the work reported in this paper.

Acknowledgments

This work was supported by the National Natural Science Foundation of China (Nos. 52371240, U1904215), Natural Science Foundation of Jiangsu Province (Nos. BK20240894, BK20200044), Changjiang Scholars Program of the Ministry of Education (No. Q2018270).

References

[1] T. Chen, F. Wang, S. Cao, et al., Adv. Mater. 34 (2022) 2201779.
[2] H. Zhou, M. Zheng, H. Pang, Chem. Eng. J. 416 (2021) 127884.
[3] G. Zhang, Y. Lu, Y. Yang, et al., J. Am. Chem. Soc. 146 (2024) 16659–16669.
[4] H. Zhou, M. Zheng, H. Tang, et al., Small 16 (2020) 1904252.
[5] H. Zhou, W. Cao, N. Sun, et al., Chin. Chem. Lett. 32 (2021) 3123–3127.
[6] H. Li, R. Zhao, W. Zhou, et al., JACS Au 3 (2023) 2107–2116.
[7] H. Zhou, X. Li, Y. Li, M. Zheng, H. Pang, Nano-Micro Lett. 11 (2019) 40.
[8] S. Gu, G. Du, Y. Su, et al., J. Colloid Interface Sci. 677 (2025) 21–29.
[9] H. Zhou, Y. Sun, H. Yang, et al., Adv. Sci. 10 (2023) 2303636.
[10] H. Zhou, S. Zheng, X. Guo, et al., J. Colloid Interface Sci. 628 (2022) 24–32.
[11] H. Yang, H. Zhou, G. Zhang, X. Guo, H. Pang, Sci. China Mater. 66 (2023) 441–469.
[12] M. Jiang, D. Jiang, X. Cao, et al., Adv. Funct. Mater. 34 (2024) 2312692.
[13] X. Cao, L. Cui, B. Liu, J. Mater. Chem. A 7 (2019) 3815–3827.
[14] J. Shen, Q. Li, Z. Cai, X. Sun, J. Liu, ACS Appl. Nano Mater. 6 (2023) 1965–1974.
[15] J. Wen, Z. Song, J. Ding, et al., J. Mater. Sci. Technol. 114 (2022) 233–239.
[16] G. Zhang, H. Yang, H. Zhou, et al., Angew. Chem. Int. Ed. 63 (2024) e202402903.
[17] Y. Bai, C. Liu, T. Chen, et al., Angew. Chem. Int. Ed. 60 (2021) 25318–25322.
[18] H.P. Li, J. Wen, S.M. Ding, et al., Nano Mater. Sci. 5 (2023) 421–428.
[19] C. Liu, Y. Bai, W. Li, et al., Angew. Chem. Int. Ed. 61 (2022) e202116282.
[20] C. Hou, Y. Wang, L. Zou, et al., Adv. Mater. 33 (2021) 2101698.
[21] Y.H. Zou, Y.B. Huang, D.H. Si, et al., Angew. Chem. Int. Ed. 60 (2021) 20915–20920.
[22] S. Lawson, M. Snarzyk, D. Hanify, A.A. Rownaghi, F. Rezaei, Ind. Eng. Chem. Res. 59 (2020) 7151–7160.
[23] L.H. Xu, S.H. Li, H. Mao, et al., Science 378 (2022) 308–313.
[24] J. Gao, X. Qian, R.B. Lin, et al., Angew. Chem. Int. Ed. 59 (2020) 4396–4400.
[25] Y. Chen, R. Gao, S. Ji, et al., Angew. Chem. Int. Ed. 60 (2021) 3212–3221.
[26] C. Zhang, L. Yuan, C. Liu, et al., J. Am. Chem. Soc. 145 (2023) 7791–7799.
[27] A. Ambrosi, M. Pumera, Chem. Soc. Rev. 45 (2016) 2740–2755.
[28] A.C. Farsheed, A.J. Thomas, B.H. Pogostin, J.D. Hartgerink, Adv. Mater. 35 (2023) 2210378.
[29] Y. Sun, L. Wang, Y. Ni, et al., Nat. Commun. 14 (2023) 1245.
[30] H. Yuk, B. Lu, S. Lin, et al., Nat. Commun. 11 (2020) 1604.
[31] H. Li, J. Liang, Adv. Mater. 32 (2020) 2070023.
[32] L. Li, J. Meng, X. Bao, et al., Adv. Energy Mater. 13 (2023) 2203683.
[33] D.K. Limberg, J.H. Kang, R.C. Hayward, J. Am. Chem. Soc. 144 (2022) 5226–5232.

[34] L. Yue, S.Macrae Montgomery, X. Sun, et al., Nat. Commun. 14 (2023) 1251.
[35] P. Zhang, I.M. Lei, G. Chen, et al., Nat. Commun. 13 (2022) 4775.
[36] Y. Bai, C. Liu, Y. Shan, et al., Adv. Energy Mater. 12 (2022) 2100346.
[37] Y.-Z. Zhang, Y. Wang, T. Cheng, et al., Chem. Soc. Rev. 48 (2019) 3229–3264.
[38] M. Zhu, Y. Huang, Q. Deng, et al., Adv. Energy Mater. 6 (2016) 1600969.
[39] J. Park, M. Lee, D. Feng, et al., J. Am. Chem. Soc. 140 (2018) 10315–10323.
[40] W. Cheng, X.F. Lu, D. Luan, X.W. (David) Lou, Angew. Chem. Int. Ed. 59 (2020) 18234–18239.
[41] D. Liu, Y. Yan, H. Li, et al., Adv. Mater. 35 (2023) 1–14.
[42] C. Zhang, L. McKeon, M.P. Kremer, et al., Nat. Commun. 10 (2019) 1795.
[43] J. Orangi, F. Hamade, V.A. Davis, M. Beidaghi, ACS Nano 14 (2020) 640–650.
[44] H. Lu, J. Hu, Y. Zhang, et al., Adv. Mater. 35 (2023) 2209886.
[45] H. Tetik, J. Orangi, G. Yang, et al., Adv. Mater. 34 (2022) 2104980.
[46] H. Wang, J. Wang, J. Tao, K. Jin, Y. Li, Nanocomposites 10 (2024) 68–77.
[47] C. Yang, X. Wu, H. Xia, et al., ACS Nano 16 (2022) 2699–2710.
[48] S. Jambhulkar, S. Liu, P. Vala, et al., ACS Nano 15 (2021) 12057–12068.
[49] B. Akuzum, K. Maleski, B. Anasori, et al., ACS Nano 12 (2018) 2685–2694.
[50] Y. Wu, D. Zhao, J. Zhang, et al., ACS Omega 6 (2021) 33067–33074.
[51] J. Fu, S.E. Taher, R.K. Abu Al-Rub, et al., Adv. Eng. Mater. 24 (2022) 2101388.
[52] G. Zhou, M. Li, C. Liu, Q. Wu, C. Mei, Adv. Funct. Mater. 32 (2022) 2109593.
[53] G. Zhou, X. Liu, C. Liu, et al., J. Mater. Chem. A 12 (2024) 3734–3744.
[54] H. Gurbuz, K. Tok, M. Gumustas, et al., FlatChem 49 (2025) 100811.
[55] Y. Li, S. Peng, R.K. Kankala, et al., Compos. Part Appl. Sci. Manuf. 163 (2022) 107182.
[56] Y. Li, R.K. Kankala, A.Z. Chen, S.B. Wang, Nanomaterials 12 (2022) 2862.
[57] K. McLellan, T. Li, Y.C. Sun, M.B. Jakubinek, H.E. Naguib, ACS Appl. Polym. Mater. 4 (2022) 8774–8785.
[58] T. Hua, H. Guo, J. Qin, et al., RSC Adv. 12 (2022) 24980–24987.
[59] Y. Dai, X. Wu, L. Li, et al., J. Mater. Chem. A 10 (2022) 11375–11385.
[60] H. Ye, Y. He, T. You, F. Xu, Adv. Funct. Mater. 35 (2025) 2413343.
[61] G. Zhu, Y. Hou, J. Lu, et al., J. Mater. Chem. A 11 (2023) 25422–25428.
[62] E. Redondo, M. Pumera, Electrochem. Commun. 124 (2021) 106920.
[63] L. Yu, W. Li, C. Wei, et al., Nano-Micro Lett. 12 (2020) 143.
[64] X. Li, H. Li, X. Fan, X. Shi, J. Liang, Adv. Energy Mater. 10 (2020) 1903794.
[65] A. Jalali, T. Gupta, V. Pakharenko, et al., Carbohyd. Polym. 352 (2025) 123252.
[66] Y. Liu, W. Geng, L. Wang, et al., Chem. Engin. J. 505 (2025) 159489.
[67] Y. Wang, X. Wang, X. Li, et al., Adv. Funct. Mater. 29 (2019) 1900326.
[68] Z. Fan, C. Wei, L. Yu, et al., ACS Nano 14 (2020) 867–876.
[69] Z. Fan, J. Jin, C. Li, et al., ACS Nano 15 (2021) 3098–3107.
[70] L. Yu, Z. Fan, Y. Shao, et al., Adv. Energy Mater. 9 (2019) 1901839.
[71] G. Shi, Y. Zhu, M. Batmunkh, et al., ACS Nano 16 (2022) 14723–14736.
[72] L. Zhong, J. Chen, Z. Ma, et al., Nanoscale 12 (2020) 24437–24449.
[73] W.Q. Ding, L. Xu, X.Y. Li, M.L. Fu, B. Yuan, ACS Appl. Mater. Interfaces 15 (2023) 49181–49194.
[74] E. Cutuli, D. Sanalitro, G. Stella, L. Saitta, M. Bucolo, Micromachines 14 (2023) 2115.
[75] S. Lawson, C. Griffin, K. Rapp, A.A. Rownaghi, F. Rezaei, Energy Fuels 33 (2019) 2399–2407.
[76] M. Chai, S. Razavi Bazaz, R. Daiyan, et al., Chem. Eng. J. 426 (2021) 130856.
[77] A.J. Young, R. Guillet-Nicolas, E.S. Marshall, et al., Chem. Commun. 55 (2019) 2190–2193.
[78] A. Pustovarenko, B. Seoane, E. Abou-Hamad, et al., Mater. Adv. 2 (2021) 2739–2749.
[79] N. Fijoł, A. Mautner, E.S. Grape, et al., J. Mater. Chem. A 11 (2023) 12384–12394.
[80] I. Pellejero, F. Almazán, M. Lafuente, et al., J. Ind. Eng. Chem. 89 (2020) 194–203.
[81] S. Lawson, A.-A. Alwakwak, A.A. Rownaghi, F. Rezaei, ACS Appl. Mater. Interfaces 12 (2020) 56108–56117.
[82] O. Halevi, J.M.R. Tan, P.S. Lee, S. Magdassi, Adv. Sustain. Syst. 2 (2018) 1700150.
[83] Z. Liu, X. Xia, W. Li, et al., Materials 13 (2020) 4403.
[84] B. Chen, R. Davies, H. Chang, et al., Addit. Manuf. 38 (2021) 101774.
[85] W. Liu, O. Erol, D.H. Gracias, ACS Appl. Mater. Interfaces 12 (2020) 33267–33275.
[86] M. Bible, M. Sefa, J.A. Fedchak, et al., 3D Print. Addit. Manuf. 5 (2018) 63–72.
[87] H. Wei, W. Chen, S. Chen, T. Zhang, X. Xiao, J. Biomater. Sci. Polym. Ed. 35 (2024) 443–462.
[88] C.-E. Choi, A. Chakraborty, H. Adzija, et al., Gels 9 (2023) 923.
[89] M.A.F. Maghsoudi, R.M. Aghdam, R.A. Asbagh, et al., Int. J. Biol. Macromol. 265 (2024) 130744.
[90] Z. Chen, S. Song, H. Zeng, et al., Chem. Eng. J. 471 (2023) 144649.
[91] Z. Li, A. Zheng, Z. Mao, et al., Int. J. Bioprinting 9 (2023) 773.
[92] S. Pal, Y.Z. Su, Y.W. Chen, et al., ACS Appl. Mater. Interfaces 14 (2022) 28247–28257.
[93] L. Saitta, E. Cutuli, G. Celano, et al., Polymers 15 (2023) 2690.
[94] T. Doan, T. Nguyen, A. Nguyen, H. Yoo, Chem. Mater. 37 (2025) 1629–1637.
[95] M. Idrees, S. Batool, W. Hu, D. Chen, Small 20 (2024) 2402266.
[96] E. Lahtinen, R.L.M. Precker, M. Lahtinen, E. Hey-Hawkins, M. Haukka, ChemPlusChem 84 (2019) 222–225.
[97] R. Li, S. Yuan, W. Zhang, et al., ACS Appl. Mater. Interfaces 11 (2019) 40564–40574.
[98] N. Qu, G. Xu, Y. Liu, et al., Adv. Funct. Mater. 35 (2024) 2402923.
[99] A. Figuerola, D.A.V. Medina, A.J. Santos-Neto, et al., Appl. Mater. Today 16 (2019) 21–27.
[100] M.C. Kreider, M. Sefa, J.A. Fedchak, et al., Polym. Adv. Technol. 29 (2018) 867–873.
[101] M.Z. Hussain, P.F. Großmann, F. Kohler, et al., Sol. RRL 6 (2022) 2200552.
[102] Z. Lyu, G.J.H. Lim, R. Guo, et al., Adv. Funct. Mater. 29 (2019) 1806658.
[103] Z. Lyu, G.J.H. Lim, R. Guo, et al., Energy Storage Mater. 24 (2020) 336–342.
[104] A.D. Salazar-Aguilar, A. Quintanilla, P. López, et al., ACS Appl. Mater. Interfaces 14 (2022) 920–932.
[105] A.I. Cherevko, I.A. Nikovskiy, Y.V. Nelyubina, et al., Polymers 13 (2021) 3881.
[106] S. Lv, K. Zhang, L. Zhu, D. Tang, Anal. Chem. 92 (2020) 1470–1476.
[107] Y. Hong, M. Wu, G. Chen, et al., ACS Appl. Mater. Interfaces 8 (2016) 32940–32947.
[108] G.J.H. Lim, Y. Wu, B.B. Shah, et al., ACS Mater. Lett. 1 (2019) 147–153.
[109] H. Thakkar, S. Eastman, Q. Al-Naddaf, A.A. Rownaghi, F. Rezaei, ACS Appl. Mater. Interfaces 9 (2017) 35908–35916.
[110] Y. Liu, J. Yang, C. Tao, et al., ACS Appl. Mater. Interfaces 14 (2022) 7184–7191.
[111] H.S. Far, M. Najafi, M. Hasanzadeh, R. Rahimi, New J. Chem. 46 (2022) 23351–23360.
[112] W. Xi, J. Zhang, Y. Zhang, et al., J. Mater. Chem. A 11 (2023) 7679–7689.
[113] A.D. Salazar-Aguilar, A. Quintanilla, S.M. Vega-Díaz, et al., Open Ceram. 5 (2021) 100047.
[114] R. Singh, G. Souillard, L. Chassat, et al., Adv. Sustain. Syst. 4 (2020) 2000059.
[115] B. Liu, J. Liu, J. Pan, et al., Sens. Actuator. B: Chem. 397 (2023) 134671.
[116] H. Shahriyari Far, M. Najafi, M. Hasanzadeh, R. Rahimi, Int. J. Environ. 105 (2025) 823–838.
[117] E.R. Kearns, R. Gillespie, D.M. D'Alessandro, J. Mater. Chem. A 9 (2021) 27252–27270.
[118] H. Zhou, G. Zhu, S. Dong, et al., Adv. Mater. 35 (2023) 2211523.
[119] H. Zhou, S. Gu, Y. Lu, et al., Adv. Mater. 36 (2024) 2401856.
[120] P. Xiao, L. Cao, H. Wang, G. Yan, Q. Chen, Surf. Interfaces 33 (2022) 102266.
[121] S. Sultan, H.N. Abdelhamid, X. Zou, A.P. Mathew, Adv. Funct. Mater. 29 (2019) 1805372.
[122] S.K. Elsaidi, M. Ostwal, L. Zhu, et al., RSC Adv. 11 (2021) 25658–25663.
[123] E. Koukouviti, A.K. Plessas, V. Pagkali, et al., Microchim. Acta 190 (2023) 274.
[124] W. Wang, Y. Xiong, R. Zhao, X. Li, W. Jia, J. Nanobiotechnology 20 (2022) 68.
[125] M. del Rio, M. Villar, S. Quesada, et al., Appl. Mater. Today 24 (2021) 101130.
[126] D. Barzallo, A. Están, N. Crespí, et al., Talanta 273 (2024) 125897.
[127] J. Liu, Y. Liu, C. Deng, et al., Adv. Mater. Technol. 7 (2022) 2101230.
[128] C.A. Grande, A. Kaiser, K.A. Andreassen, Chem. Eng. Res. Des. 192 (2023) 362–370.
[129] J. Dong, P. Li, H. Guan, et al., Inorg. Chem. Commun. 117 (2020) 107975.
[130] G.L. Denisov, P.V. Primakov, A.A. Korlyukov, V.V. Novikov, Y.V. Nelyubina, Russ. J. Coord. Chem. 45 (2019) 836–842.
[131] A. Kefayat, O. Sartipzadeh, F. Molaabasi, et al., Anal. Chem. 96 (2024) 4377–4384.
[132] Y. Zhang, Y. Su, X. Fan, et al., Adv. Opt. Mater. 11 (2023) 2300364.
[133] L. Zhang, X. Shi, Z. Zhang, et al., Angew. Chem. Int. Ed. 60 (2021) 5489–5496.
[134] E. Vlachou, A. Margariti, G.S. Papaefstathiou, C. Kokkinos, Sensors 20 (2020) 4442.
[135] L. Liu, J. Wu, S. Lv, et al., Mater. Today Bio 23 (2023) 100866.
[136] N.C. Sánchez, G.T. Palomino, C.P. Cabello, Microporous Mesoporous Mater. 348 (2023) 112398.
[137] M. Zheng, Z. Jin, Z. Ma, Z. Gu, J. Zhang, Adv. Mater. 36 (2024) 2313749.
[138] X. Zhang, Q. Zheng, H. He, T. Sun, Z. Zhang, Int. J. Hydrog. Energy 47 (2022) 9958–9968.
[139] M. Bauza, A. Figuerola, G. Palomino, C. Cabello, J. Hazardous Mater. 484 (2025) 136697.
[140] J.E. Sánchez-Velandia, F. Esteve, M. Maireles, et al., J. CO2 Util. 78 (2023) 102636.
[141] C. Shu, C. Qin, L. Chen, et al., Adv. Sci. 10 (2023) 2206875.
[142] J. Duan, Q. Li, W. Xu, X, et al., ACS Appl. Polym. Mater. 6 (2024) 1900–1910.
[143] R. Pei, L. Fan, F. Zhao, et al., J. Hazard. Mater. 384 (2020) 121418.
[144] Y. Wang, G. Rim, M. Song, et al., ACS Appl. Mater. Interfaces 16 (2024) 1404–1415.
[145] N. Bagheri, H.A.J. Al Lawati, N.A. Al Sharji, J. Hassanzadeh, Talanta 224 (2021) 121796.
[146] C. Li, S. Deng, W. Feng, et al., Small 19 (2023) 2300066.
[147] M. Idrees, S. Batool, W. Hu, D. Chen, Small 21 (2024) 2402266.
[148] C. Kokkinos, A. Economou, A. Pournara, et al., Sens. Actuator. B: Chem. 321 (2020) 128508.
[149] X. Liu, D. Zhao, J. Wang, Nano-Micro Lett. 16 (2024) 157.
[150] J. Lefevere, B. Claessens, S. Mullens, et al., ACS Appl. Nano Mater. 2 (2019) 4991–4999.
[151] A.K. Chaudhari, J. Tan, Adv. Opt. Mater. 8 (2020) 1901912.
[152] S. Lawson, Q. Al-Naddaf, A. Krishnamurthy, et al., ACS Appl. Mater. Interfaces 10 (2018) 19076–19086.
[153] J. Dhainaut, M. Bonneau, R. Ueoka, K. Kanamori, S. Furukawa, ACS Appl. Mater. Interfaces 12 (2020) 10983–10992.
[154] S. Rana, R. Sajzew, O. Smirnova, et al., Small Struct. 5 (2024) 2300346.
[155] M. Bauzá, N. Munar, A. Figuerola, G. Turnes Palomino, C.P. Cabello, J. Water Process Eng. 58 (2024) 104890.
[156] Y. Zhang, Y. Su, Y. Zhao, Z. Wang, C. Wang, Small 18 (2022) 2200514.
[157] K. Mori, T. Fujita, H. Hata, et al., ACS Appl. Mater. Interfaces 15 (2023) 51079–51088.
[158] H. Lu, J. Hu, K. Zhang, et al., Adv. Mater. 36 (2024) 2309753.
[159] S. Rana, M. Rahman, M. Zahed, et al., Nano Energy 104 (2022) 107931.
[160] L.H. Yu, X. Tao, S.R. Feng, et al., Tungsten 6 (2024) 196–211.

[161] A.K. Ipadeola, N.Z.L. Mathebula, M.V. Pagliaro, et al., ACS Appl. Energy Mater. 3 (2020) 8786–8802.
[162] H. Li, X. Li, J. Liang, Y. Chen, Adv. Energy Mater. 9 (2019) 1803987.
[163] M. Yuan, L. Wang, X. Liu, et al., Chem. Eng. J. 451 (2023) 138686.
[164] Z.P. Dong, J.J. Zhao, P.Y. Liu, Z.L. Liu, Y.Q. Wang, New J. Chem. 43 (2019) 9032–9038.
[165] A.P. Tiwari, S.S. Panicker, J.E. Huddy, et al., Adv. Mater. Technol. 9 (2024) 2301517.
[166] J.L. Ong, A.C.M. Loy, S.Y. Teng, B.S. How, ACS Omega 7 (2022) 15369–15384.
[167] L. Saitta, E. Cutuli, G. Celano, et al., Polymers 15 (2023) 4461.
[168] Y. Zhu, Q. Zhang, J. Ma, et al., Carbon Energy 6 (2024) e481.
[169] C. (John) Zhang, M.P. Kremer, A. Seral-Ascaso, et al., Adv. Funct. Mater. 28 (2018) 1705506.
[170] K. Shen, B. Li, S. Yang, Energy Storage Mater. 24 (2020) 670–675.
[171] M. Yuan, J. Shang, L. Wang, et al., Ceram. Int. 50 (2024) 11949–11955.
[172] Y. Zhu, Q. Zhang, J. Ma, et al., Carbon Ener 6 (2024) e481.
[173] T. Ito, S. Seifert, K.N. Moeller, A. Uysal, Anal. Chem. 95 (2023) 8206–8213.
[174] E. Zhang, X. Hu, L. Meng, et al., J. Am. Chem. Soc. 144 (2022) 18995–19007.
[175] A.I. Cherevko, G.L. Denisov, I.A. Nikovskii, et al., Russ. J. Coord. Chem. 47 (2021) 319–325.
[176] S.D. Perera, R.M. Johnson, R. Pawle, et al., ACS Appl. Mater. Interfaces 16 (2024) 10795–10804.
[177] L. Long, K. Xu, K. Bing Tan, et al., Chem. Eng. Sci. 266 (2023) 118278.
[178] K. Li, Y. De Rancourt, De Miménand, et al., ACS Appl. Nano Mater. 3 (2020) 2830–2845.
[179] R. Huo, C. Wang, M.Y. Wang, et al., Inorg. Chem. 62 (2023) 6661–6673.
[180] A.M. Bayoumy, A. Hessein, B.M. Ahmed, et al., J Power Sources 617 (2024) 235145.
[181] D. Tu, J. Xu, W. Yang, et al., Surf. Interfaces 30 (2022) 101873.
[182] Y. Gao, J. Ding, Adv. Mater. Technol. 8 (2023) 220063.
[183] H. Ye, Y. He, T. You, F. Xu, Adv. Funct. Mater. 35 (2025) 2413343.
[184] X. Yun, B. Lu, Z. Xiong, et al., RSC Adv. 9 (2019) 29384–29395.
[185] Y. Ren, F. Meng, S. Zhang, et al., Carbon Energy 4 (2022) 446–457.
[186] J. Yang, Q. Cao, X. Tang, et al., J Mater Chem A 9 (2021) 19649–19658.
[187] X. Lan, Z. Tian. Shen., ACS Appl. Nano Mater. 4 (2021) 6985–6994.
[188] J.J. Moyano, J. Mosa, M. Aparicio, et al., Addit. Manuf. 30 (2019) 100849.
[189] L. Liu, J. Lu, X. Long, et al., Sci. China Technol. Sci. 64 (2021) 1065–1073.
[190] Y. Zhao, F. Liu, Z. Zhao, et al., Adv. Compos. Hybrid Mater. 5 (2022) 1516–1526.
[191] Z. Wang, Z. Huang, H. Wang, et al., ACS Nano 16 (2022) 9105–9116.



Prof. Yi-Zhou Zhang received his Bachelor's degree from Nanjing University, after which he obtained a PhD from Nanjing University of Posts & Telecommunications. He is now a professor of Materials Science and Engineering at Nanjing University of Information Science and Technology (NUIST) and head of the institute of Advanced Materials and Flexible electronics in NUIST. Prof. Zhang mainly works on functional materials for printed and flexible energy storage and electronics. Due to his contributions to this field, he has been recognized as a Highly Cited Researcher by Clarivate in 2023 and 2024.



Huan Pang is a distinguished professor at Yangzhou University. He received his Ph.D. degree from Nanjing University in 2011. He is now a Young Changjiang Scholar of the Ministry of Education in China, and a senior member of the Chinese Chemical Society. He is the managing editor of EnergyChem, editorial board member of FlatChem and Rare Metals, and youth editorial board member of Nano Research and eScience among other distinguished academic journals. He has won "Best Editor Award 2021″ for his professional excellence and outstanding contribution to Nano Research. His research area mainly focuses on MOFs related materials.



Jianning Ding received his Ph.D. degree from Tsinghua University in 2001. Now, he is doing research at Yangzhou University as a professor. Prof. Jianning Ding's research interests focus on flexible mechatronics, new energy technology, and equipment functional devices, including solar cells, flexible sensors, soft robotics, and so on.